

**CHITOSAN AS NATURAL COAGULANT IN THE  
REMOVAL OF HEAVY METAL**

**JEFFREY ONG MIN HAN**

**UNIVERSITI TUNKU ABDUL RAHMAN**

**CHITOSAN AS NATURAL COAGULANT IN THE REMOVAL OF  
HEAVY METAL**

**JEFFREY ONG MIN HAN**

**A project report submitted in partial fulfilment of the  
requirements for the award of Bachelor of Chemical  
Engineering with Honours**

**Lee Kong Chian Faculty of Engineering and Science  
Universiti Tunku Abdul Rahman**

**May 2024**

## DECLARATION

I hereby declare that this project report is based on my original work except for citations and quotations which have been duly acknowledged. I also declare that it has not been previously and concurrently submitted for any other degree or award at UTAR or other institutions.

Signature : ONG

Name : Jeffrey Ong Min Han

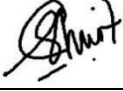
ID No. : 19UEB02109

Date : 17/05/2024

**APPROVAL FOR SUBMISSION**

I certify that this project report entitled “**CHITOSAN AS NATURAL COAGULANT IN THE REMOVAL OF HEAVY METAL**” was prepared by **JEFFREY ONG MIN HAN** has met the required standard for submission in partial fulfilment of the requirements for the award of Bachelor of Chemical Engineering with Honours at Universiti Tunku Abdul Rahman.

Approved by,

Signature :   
\_\_\_\_\_  
Supervisor : Shuit Siew Hoong  
\_\_\_\_\_  
Date : 17/05/2024  
\_\_\_\_\_

The copyright of this report belongs to the author under the terms of the copyright Act 1987 as qualified by Intellectual Property Policy of Universiti Tunku Abdul Rahman. Due acknowledgement shall always be made of the use of any material contained in, or derived from, this report.

© 2024, Jeffrey Ong Min Han. All right reserved.

## ACKNOWLEDGEMENTS

I would like to thank everyone who had contributed to the successful completion of this project. I would like to express my gratitude to my research supervisor, Dr. Shuit Siew Hoong for his invaluable advice, guidance and his enormous patience throughout the development of the research.

In addition, I would also like to express my gratitude to my loving parents and friends who had helped and given me encouragement and the necessary support to complete this project.

## ABSTRACT

Heavy metal contamination in wastewater poses serious environmental and health risks. Coagulation stands out as one of the most commonly used techniques in industry for heavy metal removal. Traditional coagulants like alum and iron chloride are unsustainable and may contribute to health issues. Chitosan, a natural coagulant derived from crustaceous shells such as crabs and shrimps, has emerged as a promising alternative. This study focuses on investigating the impact of various process parameters (chitosan dosage, pH, and the type of acid used) on chitosan's effectiveness as a coagulant in removing nickel from wastewater generated by a local electronic components manufacturer. The results suggest that chitosan alone can serve as a highly efficient primary coagulant, eliminating the necessity for supplementary aids such as alum. This is evidenced by the considerably lower removal efficiency achieved with the optimal chitosan/alum composite ratio of 0.4:0.6, which stood at only 68.62 % while pure chitosan was able to achieve a removal rate of 82.54 %. Moreover, sulfuric acid ( $\text{H}_2\text{SO}_4$ ) was identified as the most suitable acid due to its diprotic nature. Optimal conditions of using pure chitosan achieved a 96.13 % nickel removal with a chitosan dosage of 40 g/L, initial nickel concentration of 100 mg/L, and pH of 7. Interestingly, the dosage of chitosan could be reduced to 30 g/L if the wastewater underwent oxidation before the coagulation process. Further analysis using scanning electron microscopy coupled with energy dispersive X-ray spectrometry (SEM-EDX) confirmed the presence of nickel elements in the chitosan sludge, validating the efficacy of chitosan as a natural coagulant in removing heavy metals from wastewater. In summary, chitosan emerges as a promising natural coagulant for removing heavy metals, highlighting the need for further investigation in future studies.

## TABLE OF CONTENTS

<b>DECLARATION</b>		<b>i</b>
<b>APPROVAL FOR SUBMISSION</b>		<b>ii</b>
<b>ACKNOWLEDGEMENTS</b>		<b>iv</b>
<b>ABSTRACT</b>		<b>v</b>
<b>TABLE OF CONTENTS</b>		<b>vi</b>
<b>LIST OF TABLES</b>		<b>ix</b>
<b>LIST OF FIGURES</b>		<b>x</b>
<b>LIST OF SYMBOLS / ABBREVIATIONS</b>		<b>xii</b>
<b>LIST OF APPENDICES</b>		<b>xiv</b>
<b>CHAPTER</b>		
<b>1</b>	<b>INTRODUCTION</b>	<b>1</b>
1.1	Water Pollution in Malaysia	1
1.2	Heavy Metals	2
1.3	Environmental and Health Impacts	4
1.4	Problem Statement	5
1.5	Research Objectives	7
1.6	Scope of Study	7
1.7	Outline of the Study	8
<b>2</b>	<b>LITERATURE REVIEW</b>	<b>9</b>
2.1	Various Heavy Metal Removal Methods	9
2.1.1	Precipitation Methods	9
2.1.2	Membrane Filtration Method	11
2.1.3	Ion Exchange Treatment	11
2.1.4	Evaporation Method	12
2.2	Coagulation	14
2.2.1	Mechanisms of Coagulation	14
2.2.2	Coagulation Using Chemical Coagulants	15
2.3	Coagulation Using Chitosan	17



2.3.1	Structure of Chitosan	17
2.3.2	Deacetylation Degree of Chitosan	18
2.3.3	Molecular Weight of Chitosan	19
2.3.4	Advantages of Chitosan as a Coagulant	19
2.4	Study of Different Acids for Heavy Removal	21
2.5	Parameter Studies	22
2.5.1	Effect of Coagulant Dosage	22
2.5.2	Effect of Solution pH	23
2.5.3	Effect of Initial Heavy Metal Concentration	24
2.6	Wastewater Sample Analysis	24
2.7	Oxidized Wastewater Treatment	25
2.8	Sludge Volume Index Study	26
<b>3</b>	<b>METHODOLOGY AND WORK PLAN</b>	<b>27</b>
3.1	Materials and Chemicals	27
3.2	Equipment	28
3.3	Overall Flow of Study	29
3.4	Experimental Setup	30
3.5	Experimental Procedures	30
3.5.1	Preparation of Wastewater Sample	30
3.5.2	Preparation of Coagulant	30
3.5.3	Characterization of Coagulants	31
3.6	Study of Different Chitosan to Alum Ratio for Nickel Removal	31
3.7	Study of Different Acids for Nickel Removal	32
3.8	Parameter Studies	33
3.8.1	Effect of Coagulant Dosage	33
3.8.2	Effect of Solution pH	33
3.8.3	Effect of Initial Nickel Concentration	34
3.9	Wastewater Sample Analysis	34
3.10	Oxidized Wastewater Treatment	34
3.11	Sludge Volume Index	35
<b>4</b>	<b>RESULTS AND DISCUSSION</b>	<b>36</b>
4.1	Characterization of Chitosan and Alum Powders	36
4.1.1	FTIR Spectroscopy	36

4.1.2	SEM-EDX	39
4.1.3	XRD	41
4.2	Study of Different Chitosan to Alum Ratio for Nickel Removal	42
4.3	Study of Different Acids for Nickel Removal	45
4.4	Parameter Studies	46
4.4.1	Effect of Chitosan Dosage	46
4.4.2	Effect of Solution pH	47
4.4.3	Effect of Initial Nickel Concentration	48
4.5	Characterization of Chitosan Sludge	50
4.6	Oxidized Wastewater Treatment	52
4.7	Sludge Volume Index Study	56
4.8	Comparison of Optimal Parameters with Literatures	59
<b>5</b>	<b>CONCLUSIONS AND RECOMMENDATIONS</b>	<b>60</b>
5.1	Conclusions	60
5.2	Recommendations for future work	60
	<b>REFERENCES</b>	<b>62</b>
	<b>APPENDICES</b>	<b>73</b>

**LIST OF TABLES**

Table 1.1:	Malaysia Industrial Wastewater Discharge Standards (Department of Environment, 2010).	3
Table 1.2:	Toxic Effects on Heavy Metals on Human Health (Sumiahadi, Acar and Direk, 2019).	4
Table 2.1:	Advantages and Disadvantages of Physical and Chemical Methods of Heavy Metal Removal.	13
Table 3.1:	List of Chemicals and Their Specifications.	27
Table 3.2:	Chemical Properties of Heavy Metal Used in Research.	28
Table 3.3:	Model and Functions of Instruments.	28
Table 4.1:	Distribution of Elements in Pure Chitosan and Pure Alum.	40
Table 4.2:	Distribution of Elements in Chitosan/Alum Composite.	43
Table 4.3:	Distribution of Elements in Chitosan Sludge.	51
Table 4.4:	Distribution of Elements in Oxidized Sludge.	53
Table 4.5:	ICP-OES Analysis of Nickel Ions in Oxidized Wastewater.	54
Table 4.6:	Summary of SVI Calculation.	57
Table 4.7:	Comparison of Parameters.	59

## LIST OF FIGURES

Figure 1.1:	River Water Quality Status in Malaysia from 2008 to 2017 (Chai, 2020).	1
Figure 2.1:	Charge Neutralization Mechanism (Nath, Mishra and Pande, 2021).	14
Figure 2.2:	Coagulation in Removing Heavy Metal Ions (Qasem, Mohammed and Lawal, 2021).	15
Figure 2.3:	Infrared Spectra of Chitosan (Marei, 2019).	18
Figure 2.4:	Formation of Chitosan from Chitin (Wong et al., 2020).	19
Figure 3.1:	Overall Flow Diagram of Research.	29
Figure 3.2:	Diagrammatic Representation of the Experimental Setup (1) Beaker, (2) Stopwatch, (3) Magnetic Bar, (4) Hot Plate.	30
Figure 4.1:	FTIR spectrum of pure chitosan.	36
Figure 4.2:	Protonation of the Amine Group in Chitosan (Yaneva, et al., 2020).	37
Figure 4.3:	FTIR spectrum of alum.	38
Figure 4.4:	SEM Images of (a) Pure Chitosan and (b) Pure Alum.	39
Figure 4.5:	EDX Analysis for (a) Pure Chitosan and (b) Pure Alum.	40
Figure 4.6:	XRD Patterns for (a) Pure Chitosan and (b) Pure Alum.	41
Figure 4.7:	SEM Images of Chitosan/Alum Composite.	42
Figure 4.8:	EDX Analysis for Chitosan/Alum Composite.	42
Figure 4.9:	XRD Patterns for Chitosan/Alum Composite (0.4:0.6).	43
Figure 4.10:	Effect of Chitosan to Alum Ratio on the Nickel Removal (Coagulant Dosage = 40 g/L, Initial Ni Concentration = 100 mg/L, pH = 7, Contact Time = 20 minutes, Acid Type = HCl).	44
Figure 4.11:	Effect of Type of Acids on the Nickel Removal (Coagulant Dosage = 40 g/L, Initial Ni Concentration = 100 mg/L, pH = 7, Contact Time = 20 minutes).	45

Figure 4.12:	Effect of Chitosan Dosage on the Nickel Removal (Initial Ni Concentration = 100 mg/L, pH = 7, Contact Time = 20 minutes, Acid Type = H <sub>2</sub> SO <sub>4</sub> ).	46
Figure 4.13:	Effect of Solution pH on the Nickel Removal (Chitosan Dosage = 40 g/L, Initial Ni Concentration = 100 mg/L, Contact Time = 20 minutes, Acid Type = H <sub>2</sub> SO <sub>4</sub> ).	47
Figure 4.14:	Effect of Initial Nickel Concentration on the Nickel Removal (Chitosan Dosage = 40 g/L, pH = 7, Contact Time = 20 minutes, Acid Type = H <sub>2</sub> SO <sub>4</sub> ).	49
Figure 4.15:	Comparison of Chitosan Powder Before and After Treatment.	50
Figure 4.16:	SEM Images of Chitosan Sludge.	50
Figure 4.17:	Images of (a) Wastewater; (b) Oxidized Wastewater; (c) Treated Wastewater Before Settling and (d) Treated Wastewater After Settling for 30 minutes.	52
Figure 4.18:	XRD Patterns for Oxidized Wastewater.	53
Figure 4.19:	EDX Analysis for Oxidized Sludge.	53
Figure 4.20:	Effect of Chitosan Dosage on the Removal of Nickel Oxide.	55
Figure 4.21:	Treated Wastewater Sample Used for SVI Study.	56

## LIST OF SYMBOLS / ABBREVIATIONS

$C_0$	Initial heavy metal concentration, mg/L
$C_f$	Final heavy metal concentration, mg/L
$C_e$	Concentration of heavy metal at equilibrium, mg/L
SVI	Sludge volume index, mL/g
MLSS	Mixed liquor suspended solids, mg/L
$W_i$	Initial weight of filter paper, g
$W_f$	Final weight of filter paper, g
$t$	Coagulation time, min
$\lambda_{\max}$	Absorption wavelength, nm
amu	Atomic weight
Al	Aluminum
B	Boron
C	Carbon
$\text{CaCO}_3$	Limestone
CN	Cyanide
Cr	Chromium
Cu	Copper
$e^-$	Electron
$\text{H}^+$	Hydrogen ion
HCl	Hydrochloric acid
$\text{HNO}_3$	Nitric acid
$\text{H}_2\text{SO}_4$	Sulphuric acid
Hg	Mercury
$\text{H}_2\text{O}$	Water
$K_{\text{sp}}$	Solubility product
$\text{Na}_2\text{CO}_3$	Soda ash
$\text{Na}_2\text{S}$	Sodium sulphide
N	Nitrogen
Ni	Nickel
O	Oxygen
Pb	Lead

rpm	Rounds per minute
S	Sulphur
Sn	Tin
Zn	Zinc
-OH	Hydroxyl group
-NH <sub>2</sub>	Amine group
BOD	Biochemical oxygen demand
CAGR	Compound annual growth rate
COD	Chemical oxygen demand
SDG	Sustainable development goals
SVI	Sludge volume index
AAS	Atomic absorption spectroscopy
FTIR	Fourier transform infrared spectroscopy
ICP-OES	Inductively coupled plasma optical emission spectroscopy
RSM	Response surface methodology
SEM-EDX	Scanning electron microscope energy dispersive X-ray spectroscopy
UV-VIS	Ultraviolet visible spectroscopy
XRD	X-ray diffraction analysis

**LIST OF APPENDICES**

Appendix A: Preparation of Various Molarity of Acids	73
Appendix B: Preparation of Nickel Standards for ICP-OES	75
Appendix C: Calculation for Sludge Volume Index and Mixed Liquor Suspended Solids.	77



## CHAPTER 1

### INTRODUCTION

#### 1.1 Water Pollution in Malaysia

In today's rapidly evolving world, the issue of wastewater management has become increasingly prominent. With urbanization, industrialization, and population growth, the generation of wastewater and heavy metal contamination has reached staggering levels, posing a significant threat to the environment and public health.

According to the data presented in Figure 1.1, there has been a concerning trend in Malaysia where the number of rivers classified as slightly polluted or polluted has been steadily increasing since 2008. This rise is particularly alarming given the simultaneous decrease in the count of rivers categorized as clean, which has dwindled from 58 in 2015 to 46. Despite some fluctuations in the statistics, the overarching trend indicates a worrisome rise in the pollution levels of Malaysian rivers.

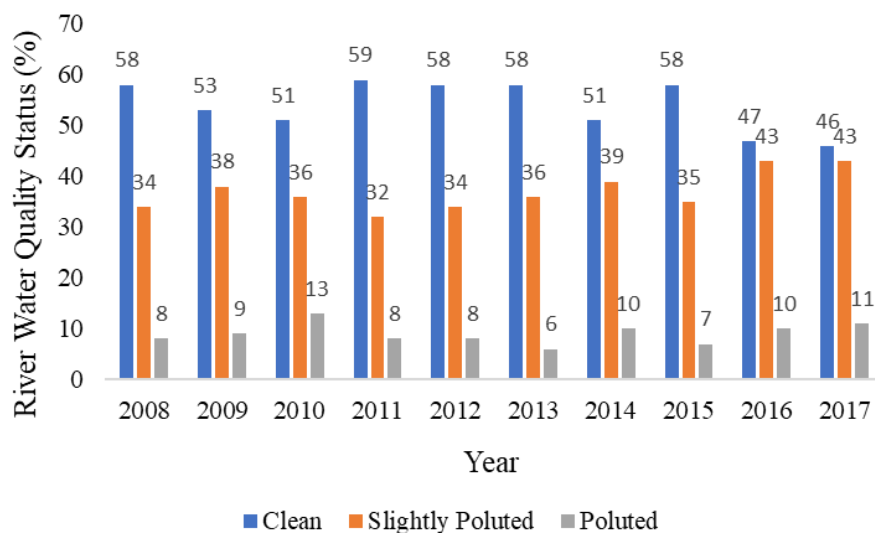


Figure 1.1: River Water Quality Status in Malaysia from 2008 to 2017 (Chai, 2020).

In Malaysia, electroplating is a very important and popular industry in various sectors, including manufacturing, automotive, electronics, aerospace,

and metal finishing. Electroplating is a liquid-based technique that entails the application of material through electrical currents. It yields a thin metal coating on the surface of an item, known as the substrate. The primary purpose of electroplating is to modify the physical attributes of an object. This method can enhance an object's durability, shield it against corrosion, enhance its visual appeal, and augment its thickness (SDC, 2017). According to a market analysis, Malaysia metal electroplating market is expected to reach USD 47.79 millions with compound annual growth rate of 4.1 % from 2018 to 2025 (ResearchAndMarkets, 2018).

The electroplating industry contributes significantly to water pollution in Malaysia through the discharge of industrial effluents. Residues generated by electroplating sectors consist of extremely hazardous cyanide (CN), metal ions with high atomic mass, organic substances, phosphorous, solid particles in suspension, pigmentation, and various other compounds, all of which are released into river streams (Department of Environment, 2010). The presence of metal ions in wastewater from the electroplating industry renders the water highly poisonous and corrosive. According to the Department of Statistic Malaysia, the country has been making progress in several sustainable development goals (SDG) such as goal 12 (responsible consumption and production) in recent years. Coupled with SDG3 (good health and well-being), it is necessary to eliminate these detrimental heavy metals to avoid their absorption by plants, animals, and even humans.

## **1.2 Heavy Metals**

Heavy metals are metallic elements characterized by an atomic density exceeding 5 g/cm<sup>3</sup> which can be naturally occurring or can be released into the environment through industrial processes or improper disposal of waste (Tchounwou, et al., 2012). Among the typical heavy metals found in wastewater are lead, mercury, chromium, nickel, copper, and zinc (Kinuthia, et al., 2020).

Electroplating processes generate a significant quantity of wastewater containing heavy metals due to processes like metal surface cleaning, rinsing, and the disposal of used plating baths. When objects are removed from the plating bath, a considerable amount of the plating solution clings to them,

leading to the loss of valuable heavy metals. These metals are then carried into subsequent rinse baths. As a result, the rinse water becomes polluted, potentially containing high levels of heavy metals. Unlike organic pollutants, heavy metals exhibit non-biodegradable characteristics and tend to accumulate within living organisms. Numerous heavy metal ions are recognized for their potential toxicity and carcinogenic properties. If left untreated, the release of such substances into the environment can potentially cause adverse impacts on the well-being of humans and other living beings (Teng and Chang, 2011). Table 1.1 below shows the Malaysia industrial wastewater discharge standards.

Table 1.1: Malaysia Industrial Wastewater Discharge Standards (Department of Environment, 2010).

Parameter	Unit	Standard	
		A	B
Temperature	°C	40	40
pH	-	6.0 – 9.0	5.5 – 9.0
BOD <sub>5</sub> at 20 °C	mg/L	20	50
COD	mg/L	50	100
Suspended Solids	mg/L	50	100
Mercury	mg/L	0.005	0.05
Cadmium	mg/L	0.01	0.02
Chromium, Hexavalent	mg/L	0.05	0.05
Arsenic	mg/L	0.05	0.1
Cyanide	mg/L	0.05	0.1
Lead	mg/L	0.1	0.5
Chromium, Trivalent	mg/L	0.2	1.0
Copper	mg/L	0.2	1.0
Manganese	mg/L	0.2	1.0
Nickel	mg/L	0.2	1.0
Tin	mg/L	0.2	1.0
Zinc	mg/L	1.0	1.0
Boron	mg/L	1.0	4.0
Iron	mg/L	1.0	5.0
Phenol	mg/L	0.001	1.0
Free Chlorine	mg/L	1.0	2.0
Sulphide	mg/L	0.5	0.5
Oil and Grease	mg/L	-	10.0

### 1.3 Environmental and Health Impacts

Heavy metals are extremely harmful substances that can cause adverse impacts on both human well-being and the natural environment as heavy metals are elemental in nature, they are resistant to decomposition and thus endure in the environment. In contrast to many organic pollutants that ultimately decompose into carbon dioxide and water, heavy metals have a tendency to build up over time, particularly in river, estuarine, and sediment environments (APIS, 2016). Different heavy metals have different degree of harm to the environment and living beings.

Heavy metal contamination in water bodies can lead to the contamination of aquatic ecosystems, impacting fish and other organisms. This contamination can cause reproductive abnormalities, genetic mutations, and even death in aquatic life (Jarup, 2003). Moreover, when heavy metals enter the soil, they can be absorbed by plants, leading to reduced crop yields and food contamination. This poses a significant threat to both agricultural productivity and food safety (Rajoria, et al., 2022).

Table 1.2: Toxic Effects on Heavy Metals on Human Health (Sumiahadi, Acar and Direk, 2019).

Heavy Metal	Toxic Effects	EPA Regulatory Limit (ppm)
Nickel	Dermatitis, eyes, nose, throat and lung irritation, nausea, asthma, cancer	0.20
Chromium	Hair loss, nausea, cancer	0.10
Copper	Brain and kidney damage, liver malfunction, haemolysis	1.30
Zinc	Depression, lethargy, neurological disorder, skin irritation and corrosion	0.50
Lead	Retardation in brain development, neurological damage, and gastrointestinal damage	15.00
Mercury	Anxiety, fatigue, insomnia, loss of memory, neurological disorder	2.00

Table 1.2 lists out some of the common heavy metals in electroplating wastewater and their toxic effects on human health. Heavy metals have the ability to bioaccumulate in the human body, meaning that even small exposures over time can result in toxic levels. Each heavy metal has its own set of health risks. For instance, exposure to lead can result in neurological harm, cognitive deficits, and developmental setbacks, particularly in children. Mercury exposure is known to affect the nervous system, causing tremors, memory loss, and even neurological disorders. Nickel exposure has been linked to dermatitis, irritations, and increased cancer risk. Hence, it's crucial not to underestimate or overlook the dangers and threats posed by heavy metal contamination.

#### **1.4 Problem Statement**

Currently, the treatments plant in Malaysia adopt techniques like membrane filtration, adsorption, and electrooxidation to remove heavy metal from wastewater (Zhou, et al., 2023). Nonetheless, these approaches have their limitations and drawbacks. As an example, fouling and membrane clogging might occur during filtration processes, thereby reducing the membrane's permeability and efficiency. Fouling necessitates more frequent cleaning and maintenance, increasing operational costs and potentially affecting the longevity of the membranes (Xiang, et al., 2022). Other than that, conventional wastewater treatment like electrooxidation can be costly and can generate a huge amount of sludges.

Coagulation is a popular and cost-effective method for effectively removing heavy metals from wastewater, known for its versatility and efficiency. The process removes heavy metal from wastewater by manipulating electrostatic charges of particles suspended in water. In this process, small particles, turbidity, and bacteria are transformed into larger flocs, which can exist as precipitates or suspended particles. These flocs are then treated to ensure their easy removal in subsequent processes (Toprak Home Page, 2006). To facilitate coagulation, a positive source is needed to neutralize the negative surface charges to destabilize particles so they can coagulate into larger particles. One of the most commonly used coagulants is alum as it is the least expensive coagulant available (Water World, 2001).

Despite its cheap price, there are some disadvantages associated with the use of alum in removing heavy metals such as the formation of sludge. Not only that, alum's effectiveness also is heavily dependent on the pH of the wastewater. Adjusting and maintaining the pH within the optimal range may require additional chemical dosing and monitoring, increasing operational complexity. In relation to health implications, the release of aluminum from alum can lead to health conditions such as Alzheimer's disease.

Due to growing emphasis on reducing the use of synthetic chemicals in wastewater treatments and promoting sustainable alternatives, scientists have been exploring alternative methods, and one of these approaches is to replace alum with chitosan as a natural coagulant in heavy metal removal. Chitosan is obtained from chitin, which is primarily sourced from the rigid exoskeletons of crustaceans and certain fungi's cell walls (Molly, 2021). Some of the advantages of using chitosan as natural coagulant are of its extensive surface area and strong adsorption capacity, ease of regeneration and biodegradability (Hesami, Bina and Ebrahimi, 2014). Since chitosan as natural coagulant is relatively new compared to other alum-based or iron-based coagulants, various studies need to be conducted to determine the most favourable operating conditions and fully utilize the potential of chitosan (Haripriyan, Gopinath and Arun, 2022).

Additionally, it's important to investigate various types of acids for dissolving chitosan in the coagulation process. For instance, acids like hydrochloric acid and sulfuric acid differ in strength (pKa values), influencing pH and subsequently affecting the charge and size of coagulated particles. The cost and availability of these acids can vary greatly (ChemREADY, 2023). In short, examining different acids helps in choosing cost-effective solutions that maintain the efficiency and safety of the coagulation process.

## 1.5 Research Objectives

The objectives of this research are:

- i. To investigate the effect of different chitosan to alum ratio and different acid type (hydrochloric acid, sulphuric acid and nitric acid ) in the removal of nickel ion.
- ii. To study and optimize the process parameters (coagulant dosage, pH of the solution and initial nickel ion concentration) in the nickel ion removal using chitosan.
- iii. To investigate the removal efficiency of chitosan in pre-oxidized nickel ion contaminated wastewater.
- iv. To study and determine the sludge volume index (SVI) of coagulation process using chitosan.

## 1.6 Scope of Study

Chitosan will be used as the standalone coagulant and as a coagulant aid in heavy metal removal due to its biodegradable, non-toxic, antimicrobial, and antibacterial properties. The heavy metal removal efficiency will be characterized by using various methods such as inductively coupled plasma optical emission spectroscopy (ICP-OES) and atomic absorption spectroscopy (AAS). Other than that, fourier transform infrared spectroscopy (FTIR), X-ray diffraction (XRD) and scanning electron microscope energy dispersive X-ray spectroscopy (SEM-EDX) will also be utilized.

Subsequently, experiments will be conducted to assess variations in heavy metal removal efficiency under varying condition. These are the effect of different chitosan to alum ratio, coagulant dosage, pH of the wastewater, and initial heavy metal concentration. Subsequently, experiments will be conducted to examine the impact of hydrochloric acid (HCl), sulfuric acid (H<sub>2</sub>SO<sub>4</sub>), and nitric acid (HNO<sub>3</sub>) on both pH adjustment in wastewater and the dissolution of coagulants.

Additionally, there will be an investigation into the treatment of oxidized wastewater, aiming to address its specific challenges effectively. Moreover, a detailed analysis of the sludge volume index (SVI) will be conducted to better understand the settling characteristics of the sludge in wastewater treatment processes.

## **1.7 Outline of the Study**

The report is structured into five chapters. In Chapter 1, the focus is on water pollution in Malaysia, particularly within the heavy metal and electroplating industry, along with the associated impacts to the environment and health. The problem statement outlines the necessity of the study, while the objectives delineate the issues to be addressed through the research. The scope of study provides detailed insight into the objectives and the research conducted.

Chapter 2 comprises a review of relevant literature on heavy metal removal methods, coagulation, the fundamental properties of alum and chitosan, as well as the mechanisms underlying coagulation. The literature also identifies key factors influencing coagulation processes.

Chapter 3 elucidates the research methodology, detailing the materials and chemical reagents used. It provides a comprehensive account of the preparation of chitosan and outlines the experimental setup and methods employed for characterizing the coagulant.

In Chapter 4, the results and discussions of the study are presented. This section encompasses the characterization of the coagulants, a process study on factors affecting coagulation, and an analysis of the sludge volume index.

Chapter 5 serves as a summary of the entire study, offering conclusions drawn from the research findings and recommendations for future work based on these conclusions.



## CHAPTER 2

### LITERATURE REVIEW

#### 2.1 Various Heavy Metal Removal Methods

In the past few decades, there has been a concerted effort to innovate and refine a range of specialized treatment procedures with the aim of eliminating heavy metals from wastewater effectively and economically prior to discharge into the environment. The methods developed include precipitation, membrane filtration, ion exchange treatment and many other methods.

##### 2.1.1 Precipitation Methods

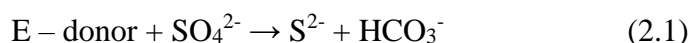
Precipitation is a commonly employed and efficient technique for eliminating heavy metals from wastewater and industrial discharge. Precipitation involves converting soluble metals into solid forms within a solution. In the context of metal removal, the goal is to precipitate as much solid metal as possible to facilitate its removal from the wastewater (Sarup, et al., 2021). There are mainly two methods of precipitation, chemically or biologically.

Chemical precipitation operates on the principle of saturation. When a solution reaches a point of saturation, exceeding the solubility product ( $K_{sp}$ ), a metal will precipitate. The precipitation process involves several stages: nucleation, nucleus growth, and aggregation or crystallization. Successful precipitation hinges on factors like solution pH and the metal concentration. Different types of metals can be reclaimed as oxides/hydroxides, sulphides, carbonates, or phosphates. To achieve this, various chemical agents are employed. For instance, metals can undergo precipitation as oxides or hydroxides by utilizing substances such as sodium hydroxide, calcium hydroxide, magnesium hydroxide, magnesium oxide, and calcium carbonate (Dahman, 2017). Sulphides are formed with substances like sodium sulphide ( $\text{Na}_2\text{S}$ ) while carbonates can be produced using soda ash ( $\text{Na}_2\text{CO}_3$ ) or limestone ( $\text{CaCO}_3$ ) (Chen, et al., 2018).

Chemical precipitation serves as a straightforward and effective technique to extract metals from highly concentrated leachates. Nevertheless, its efficiency is closely tied to pH, and it struggles with leachates that contain

low concentrations of soluble metals, often leading to the creation of harmful sludge.

On a different note, biological precipitation involves microorganisms that can either directly incorporate metals into their metabolism or indirectly facilitate precipitation through the production of metabolites that react with dissolved metals (Janyasuthwong, 2017). One extensively studied and applied method is metal precipitation through sulphate reduction. This method utilizes sulphate-reducing bacteria, which use a carbon source or hydrogen as electron donors and sulphate as electron acceptors, leading to the production of sulphide under anaerobic conditions. The formed sulphide then interacts with metal ions, resulting in the formation of solid metal sulphide precipitates.



Various types of waste materials containing metals, such as biosolids, mining leachate, and landfill leachate, are enriched with sulphate. This characteristic enables the utilization of the sulphate reduction process for the purpose of metal precipitation. Metal sulphides, including cobalt, copper, iron, nickel, and zinc sulphides, exhibit relatively low solubility constants. This makes the sulphate reduction method a feasible and attractive option for precipitating, reclaiming, and reusing these particular metals. The efficacy of sulphate reduction-based precipitation has already been demonstrated in effectively recovering metals from acid mine drainage (Kikuchi and Tanaka, 2012). Another avenue for metal precipitation involves microorganisms engaging in a process called bio reductive precipitation. In this approach, microorganisms incorporate metals into their metabolic processes, yielding precipitation. As an example, uranium (VI) can be converted to uranium (IV) by bacteria specialized in uranium reduction. Similarly, selenite and selenate can be transformed into elemental selenium through the actions of selenite-reducing bacteria, and tellurite can undergo conversion into elemental tellurium through the action of tellurite-reducing microorganisms.

When compared to chemical precipitation, biological precipitation offers several advantages. These encompass reduced expenses, the elimination of sulphate in waste with sulphate content, suitability for leachates containing low metal concentrations, selective removal of specific metals, and improved settling, thickening, and dewatering of metal sulphide sludges in sulphate-containing waste. However, its performance is still heavily dependent on several factors, such as temperature, pH, ionic strength, and presence of impurities.

### **2.1.2 Membrane Filtration Method**

Membrane filtration is a physical separation method for filtering specific substances from a medium through a thin semi-permeable layer called membrane. Different types of membrane filtration, including microfiltration, , nanofiltration, and reverse osmosis, can be employed to separate organic and inorganic contaminants from wastewater based on their size. This separation is achieved by applying a transmembrane pressure gradient.

When treating electroplating wastewater, microfiltration, and ultrafiltration, which have pores sizes of 0.1 – 1 and 0.01 – 0.1  $\mu\text{m}$ , respectively, are two of the most popular types of membrane filtration. However, it has not drawn enough attention in heavy metal removal because of its low removal ability. Due to their large pore size, they are not completely impermeable to heavy metals (Xiang, et al., 2022).

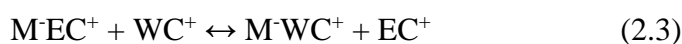
The disadvantages of membrane filtration are the high cost of the membrane construction and slow filtration speed. Generally, ceramic membranes are used for removing heavy metal in wastewater but due to its fragile feature, the membrane can crack easily (Sourav, 2023).

### **2.1.3 Ion Exchange Treatment**

The ion exchange technique is a reversible chemical process used to replace harmful metal ions with environmentally benign ones. This method entails extracting metal ions from wastewaters by attaching it to an inert solid particle, effectively exchanging the solid particle's cation with the heavy metal ion (Al-Enezi, Hamoda and Fawzi, 2004). The solid ion-exchange particles can be made from natural sources like inorganic zeolites or synthetically produced

materials like organic resins. This method is capable of removing specific heavy metal ions like lead, cadmium, nickel and copper ions from wastewater.

The process of ion exchange for removing metals can be described through the following reaction: the ion exchange particle, with an ion exchanger represented as  $M^-EC^+$  (where  $M^-$  and  $EC^+$  are the fixed anion and exchange cation, often using  $Na^+$  or  $H^+$  as exchange cations), exchanges its cation ( $EC^+$ ) with the cation in the wastewater ( $WC^+$ ).



One of the drawbacks of ion exchange is that when managing highly concentrated heavy metal wastewater, ion exchange materials become saturated with adsorbed metals rapidly. This necessitates frequent replacement or cycles of metal ion desorption (Fu, et al., 2022). Therefore, further research is required to investigate the stability and reusability of the ion exchange method.

#### **2.1.4 Evaporation Method**

Evaporation stands as another prevalent technique employed within the electroplating sector for wastewater treatment. Its primary purpose is to concentrate diluted waste streams for the eventual recovery of metals. This thermal separation method involves the removal of water from wastewater through evaporation, resulting in the creation of both concentrated material and water vapor. The concentrated substance, containing a notable concentration of heavy metals, is typically transported off-site for either metal reclamation or disposal. On the other hand, the vaporized water, free from contaminants, is condensed into purified water and reintroduced into the process baths for reuse. This approach effectively reduces the overall volume of wastewater produced by an electroplating facility, leading to a substantial reduction in the expenses associated with treatment and disposal.

Two commonly employed types of evaporators are atmospheric and vacuum evaporators. Atmospheric evaporators use heat to convert water into vapor under regular pressure conditions, while vacuum evaporators vaporize water at lower temperatures under reduced pressure. Regardless of the specific

type, the evaporation process demands a significant amount of energy and may not be economically viable if not operated at an optimal evaporation rate. Generally, the feasibility of utilizing an evaporator hinge on the associated energy costs. Table 2.1 below summarizes the advantages and disadvantages of conventional treatment methods.

Table 2.1: Advantages and Disadvantages of Physical and Chemical Methods of Heavy Metal Removal.

<b>Treatment Methods</b>	<b>Benefits</b>	<b>Drawbacks</b>
Precipitation	<ul style="list-style-type: none"> <li>• With a solid track record of success in various industries</li> <li>• Simple operation</li> <li>• Low energy consumption</li> <li>• Low capital cost</li> <li>• Not metal selective</li> </ul>	<ul style="list-style-type: none"> <li>• Production of substantial quantity of sludge</li> <li>• Extra operating cost for disposing sludge</li> </ul>
Membrane Filtration	<ul style="list-style-type: none"> <li>• Compact system</li> <li>• High efficiency</li> </ul>	<ul style="list-style-type: none"> <li>• Susceptible to membrane clogging, scaling, fouling and degradation.</li> <li>• High capital and maintenance cost</li> <li>• High operating cost</li> </ul>
Ion Exchange	<ul style="list-style-type: none"> <li>• Metal selective</li> <li>• High metal removal efficiency</li> <li>• No sludge generation</li> </ul>	<ul style="list-style-type: none"> <li>• Susceptible to resin fouling and degradation</li> <li>• Limited applications</li> </ul>
Evaporation	<ul style="list-style-type: none"> <li>• High purity of distillate water produced.</li> <li>• No chemical consumption</li> <li>• Elimination or reduction of effluent volume</li> </ul>	<ul style="list-style-type: none"> <li>• High energy consumption</li> <li>• Distillate water produced may be contaminated</li> </ul>

## 2.2 Coagulation

### 2.2.1 Mechanisms of Coagulation

Coagulation is a common method used by wastewater treatment plants that utilizes chemicals or electric currents to form clumps of particles that are sized  $< 10 \mu\text{m}$  (colloidal particles) or between  $10 - 100 \mu\text{m}$  (turbidity) that can be removed from wastewater (Eric, 2022). The process destabilizes the colloids by using chemicals called a coagulant. A coagulant is usually high valence. Some of the commonly used coagulant in industries include aluminum sulfate or alum, ferric sulfate, and magnesium chloride (Teng and Chang, 2011). This approach is frequently combined with techniques such as filtration, disinfection, and sedimentation to eliminate specific impurities, particularly heavy metals, from electroplating wastewater (Brian, 2022).

The mechanism of coagulation in removing heavy metal from wastewater is based on the principle of neutralizing the electrical charges of the metal ions and the colloidal particles in the solution, and forming larger aggregates that can be separated by filtration or sedimentation (ChemREADY, 2018). When the coagulants are added into the wastewater it dissociates and form positively charged metal hydroxide or metal oxide ions. Heavy metal ions and other particles in the wastewater typically carry a negative charge due to their surface properties. The positively charged metal hydroxide or metal oxide ions from the coagulant neutralize the negative charges on these particles (Lara, Rodríguez and Peñuela, 2016). The neutralized particles start to collide and adhere to each other, forming larger and heavier aggregates called flocs (Jon, 2022).

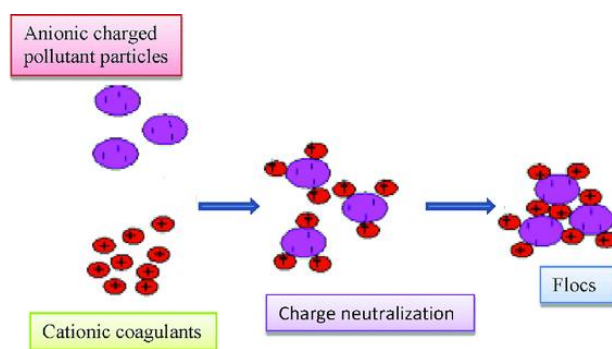


Figure 2.1: Charge Neutralization Mechanism (Nath, Mishra and Pande, 2021).

These flocs entrap heavy metal ions and other impurities within their structure. The formed flocs are now significantly larger and heavier than individual particles, making them easier to settle out or separate from the water. The wastewater is allowed to sit in a settling basin or tank, where flocs settle to the bottom due to gravity. Alternatively, flotation can be used, where tiny air bubbles are introduced to attach to the flocs and float them to the water's surface. After settling or flotation, the clarified water at the top is separated from the settled flocs or floated particles at the bottom or surface. This clarified water is further treated or discharged, while the concentrated sludge containing the removed heavy metals and other impurities is collected and treated for disposal or recovery of valuable materials.

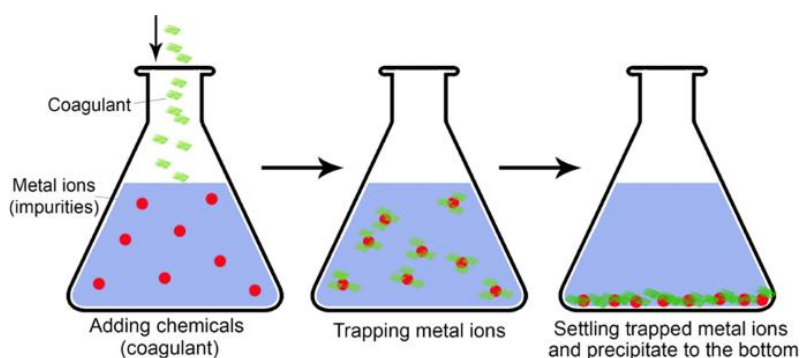


Figure 2.2: Coagulation in Removing Heavy Metal Ions (Qasem, Mohammed and Lawal, 2021).

### 2.2.2 Coagulation Using Chemical Coagulants

Chemical coagulants, which are synthetic materials, find widespread application in modern wastewater treatment facilities. These coagulants, including substances like aluminum sulfate, ferric chloride, and polyaluminum chloride, are proficient in eliminating heavy metals through the formation of insoluble metal hydroxides or complexes. These resultant compounds can be conveniently separated through settling or filtration processes (Al Kindi, Gomaa and Abd ulkareem, 2020). However, the use of chemical coagulants presents similar issues found in other treatment methods, including high treatment costs, substantial sludge production, and potential health risks from residual chemicals in the treated water.

A drawback associated with the utilization of chemical coagulants is the volume of sludge generated post-treatment. While sludge is a common byproduct in various treatment methods, introducing chemicals into incoming solutions can notably contribute to its production. The sludge generated by chemical coagulation can reach up to 0.5 % of the volume of the treated water. Following water treatment, the generated sludge usually undergoes a dewatering phase before being disposed of at suitable sites. Notably, sludge produced by specific chemical additives like alum can cause corrosion, acidification, and toxicity to aquatic life or soil organisms (Genesis Water Tech, 2019). Sludge is known for being difficult to clean, and inadequate cleaning can lead to process complications. Consequently, disposing of sludge can be a costly and demanding endeavor, particularly in regions where options like landfills or incineration are scarce (Barrera-Díaz, Balderas-Hernández and Bilyeu, 2018).

Next, chemical coagulants have high operational costs and environmental impacts. Chemical coagulants are usually synthetic substances that are manufactured from non-renewable resources and require a lot of energy and chemicals to produce. According to a study by Bazrafshan, et al. (2016), it has been estimated that the cost of chemical coagulants required for treating dairy wastewater was 0.18 USD/m<sup>3</sup>, which accounted for 40 % of the total treatment cost. It was noted that the costs still didn't include the additional sludge treatment cost (Bazrafshan, et al., 2016). Hence, chemical coagulants could pose notable financial challenges for wastewater treatment facilities, particularly in developing nations where the accessibility and affordability of such chemicals are constrained (Das, et al., 2023).

The utilization of traditional chemical coagulants for wastewater treatment is receiving significant focus. Concerns about the long-term impact on human well-being and the environment resulting from the creation of non-degradable sludge by-products are currently emerging as prominent subjects. Shifting from chemical to natural coagulants presents a viable approach to mitigating the mentioned downsides (Bahrodin, et al., 2021). According to Nguyen, et al. (2023), the natural coagulant derived from cassia fistula seeds exhibited greater effectiveness in eliminating heavy metals compared to polyaluminum chloride. This natural coagulant achieved a metal ion removal



rate of more than 80 % under ideal circumstances, which included a pH of 5.0, a metal ion concentration of 25 ppm, and recommended dosages of 0.8 g/L for  $Zn^{2+}$  and 1.6 g/L for  $Ni^{2+}$  (Nguyen, et al., 2023). The reason behind this lies in the fact that many coagulants derived from natural sources encompass biopolymers possessing reactive sites that can adsorb heavy metals. This characteristic renders them more efficient, and discerning compared to certain chemical coagulants, which result in the creation of insoluble metal hydroxides or oxides (Alazaiza, et al., 2022).

## **2.3 Coagulation Using Chitosan**

### **2.3.1 Structure of Chitosan**

In recent years, the wastewater industries have been searching for a greener alternative to replace chemical coagulant in removing heavy metal from wastewater. This is due to the increasing emphasis on promoting green technology and reducing the reliability on chemical synthetic materials. Laboratory studies have shown that chitosan is an outstanding alternative to chemical coagulants due to its versatility and ease of handling. Compared to other green coagulants like moringa oleifera seeds, chitosan has demonstrated greater consistency and has been more extensively researched (Kučera and Hofmanová, 2020). Furthermore, chitin, which chitosan are derived from, ranks among the most abundant natural polymers globally. Chitosan has many applications in water and wastewater treatment, such as coagulation, flocculation, adsorption, and membrane filtration. Chitosan can remove various pollutants from water, such as suspended solids, organic matter, heavy metals, dyes, phosphates, oils, and microorganisms (Khairul, et al., 2021).

Chitosan is a naturally occurring polymer obtained from chitin, which is found from marine organisms inhabiting seawater, including the shells of shrimp, crabs, and lobsters. This long-chain carbohydrate molecule is not water-soluble and remains insoluble in organic solvents. However, it exhibits solubility in the majority of weak acids ( $pH < 6.5$ ) and carries positively charged moieties. When introduced into acidic solutions, it has the ability to transform glucosamine units into a soluble state, denoted as R-NH<sub>3</sub>.

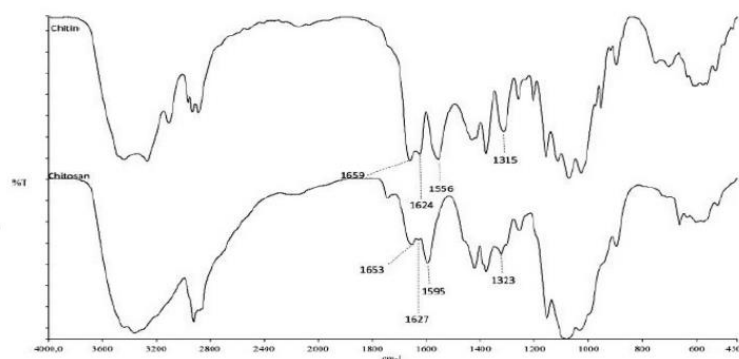


Figure 2.3: Infrared Spectra of Chitosan (Marei, 2019).

Based on the Figure 2.3, it is evident that there are three distinct absorption bands present: the absorption peaks corresponding to the amide (I) bands of chitosan can be identified around 1655-1630  $\text{cm}^{-1}$ , while chitin's amide (II) bands are observed at approximately 1560  $\text{cm}^{-1}$ . The absorption bands attributable to -OH groups can be found at 3450  $\text{cm}^{-1}$ . Additionally, chitosan's backbone incorporates highly reactive amino (-NH<sub>2</sub>) and hydroxyl (-OH) groups. This distinctive composition renders chitosan a potent adsorbent material for metal ions (Nath, Mishra and Pande, 2021).

### 2.3.2 Deacetylation Degree of Chitosan

Chitosan can be derived from chitin through a process called deacetylation. It is a process that is used to remove the acetyl group from chitin, thereby forming chitosan. The deacetylation process of chitin into chitosan is not entirely finished. By managing the reaction conditions, it becomes achievable to procure chitosan with varying degrees of acetylation (Fernandes, et al., 2015). The deacetylation degree of chitosan refers to the extent of deacetylation of the chitin molecule, resulting in amino groups that can be protonated and carry a positive charge. The positive charges on chitosan interact with negatively charged particles, including heavy metal ions, facilitating their neutralization and subsequent aggregation into flocs (John, et al., 2020). Besides that, higher deacetylation degrees lead to higher charge densities on chitosan's carbon chain molecules, which can enhance its coagulation performance. The degree of deacetylation significantly impacts chitosan's solubility, viscosity, crystallinity, ion exchange capacity, and its ability to cause flocculation (Li, Elango and Wenhui, 2020).

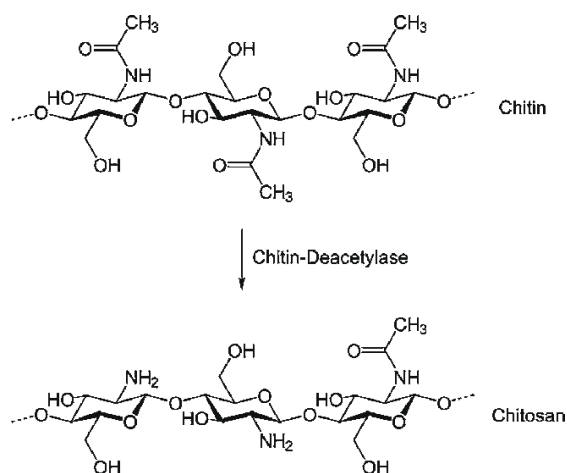


Figure 2.4: Formation of Chitosan from Chitin (Wong et al., 2020).

### 2.3.3 Molecular Weight of Chitosan

The molecular weight of chitosan affects its ability to form flocs with suspended particles in the water. Generally, higher molecular weight chitosan molecules have higher viscosity, charge density, and bridging ability, which can enhance the coagulation and flocculation of suspended particles and dissolved pollutants such as heavy metals (Lichtfouse, et al., 2019). Furthermore, larger flocs formed with higher molecular weight chitosan are more likely to settle or float effectively, aiding in the removal of heavy metal-loaded flocs from the water. However, higher molecular weight chitosan might be more shear-sensitive, meaning that excessive mixing or turbulence could break down the flocs, reducing coagulation efficiency (Khairul, et al., 2021).

In summary, the molecular weight and deacetylation degree of chitosan are critical factors in determining its performance as a coagulant for heavy metal removal. Careful selection and optimization of these parameters are essential for achieving efficient heavy metal removal during coagulation.

### 2.3.4 Advantages of Chitosan as a Coagulant

There are several reasons why chitosan is a solid replacement for chemical coagulants, such as chitosan is biodegradable and biocompatible, meaning it can break down naturally and does not harm live organisms. Chemical coagulants, such as aluminium or iron salts, may cause environmental problems such as corrosion, acidification, and toxicity to aquatic life and soil organisms (Alazaiza, et al., 2022).

Chitosan can also be used as a coagulant aid for enhancing the effectiveness of heavy metal removal with chemical coagulants. According to research by Bina, et al. (2009), it was found out that the turbidity removal efficiency had increased from 74.3 % to 98.2 % when chitosan was used as a coagulant aid with alum as the main coagulant. Besides that, the residual of  $Al^{3+}$  ions were decreased (Bina, et al., 2009). Further validation for this statement comes from Lara, et al. (2016), whose research indicated that employing chitosan as the sole coagulant for zinc and copper removal yielded fewer effective results in comparison to alum and ferric chloride. Nonetheless, when chitosan was employed as a coagulant aid, the levels of remaining aluminium and iron ions saw considerable reduction, thereby mitigating the potential adverse impacts they could pose (Lara, Rodríguez and Peñuela, 2016).

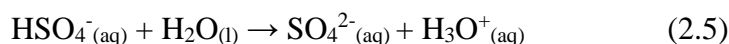
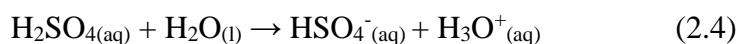
According to another study from Bina, et al. (2014), it was found out that chitosan in removal of heavy metal produced less sludge than ferric chloride, meaning it can increase the environmental sustainability and reduce the sludge handling cost (Hesami, Bina and Ebrahimi, 2014). Chitosan has the ability to minimize sludge generation by directly causing suspended and colloidal particles in wastewater to coalesce, eliminating the requirement for metal-based coagulants (Lichtfouse, et al., 2019). Furthermore, chitosan can optimize sludge dewatering by creating a porous and sturdy framework that facilitates the efficient drainage of water. As a result, chitosan emerges as a sustainable and effective substitute for reducing sludge while remaining environmentally conscious (Fan, et al., 2019).

In summary, chitosan offers several key benefits, including its non-toxicity, lack of adverse effects on human health, high molecular weight as a linear cationic polymer, and biodegradability. Utilizing chitosan as a primary coagulant has the potential to reduce the expenses associated with wastewater treatment. Additionally, it serves as an environmentally friendly coagulant with no harmful repercussions. However, chitosan also has some limitations and challenges, such as variable quality depending on the source, its possible allergic reactions in some people, and its regulatory status in different countries. Therefore, more research and development are needed to optimize its properties and applications.

## 2.4 Study of Different Acids for Heavy Removal

Accurate pH modification is essential in influencing the effectiveness of coagulation for heavy metal removal. Consequently, the utilization of acids is imperative to adjust the pH of solutions (ChemREADY, 2023). In modern industrial wastewater treatment, two of the most commonly used acids are hydrochloric acid (HCl) and sulphuric acid (H<sub>2</sub>SO<sub>4</sub>). Nevertheless, even though HCl is the more potent acid owing to its pK<sub>a</sub> value of -6.3, which is lower than H<sub>2</sub>SO<sub>4</sub>'s value of -2.8, H<sub>2</sub>SO<sub>4</sub> is favored for pH modification in wastewater treatment. pK<sub>a</sub> represents a numerical value that characterizes the acidic nature of a specific molecule. It quantifies the potency of an acid by gauging the degree to which a proton is bound to a Bronsted acid. A lower pK<sub>a</sub> value signifies a more potent acid, indicative of its heightened capability to relinquish protons (BYJU'S, 2023).

H<sub>2</sub>SO<sub>4</sub> functions as a diprotic acid, capable of contributing two H<sup>+</sup> ions per individual molecule. When it enters water, it undergoes dissociation, resulting in the formation of hydronium ions (H<sub>3</sub>O<sup>+</sup>) and sulfate ions (SO<sub>4</sub><sup>2-</sup>) (Sajid, 2023). The equations are expressed as below:



Apart from this, when employed in a 98 % concentration, only a minor quantity of H<sub>2</sub>SO<sub>4</sub> is needed to attain equivalent outcomes compared to alternative acids like HCl. Moreover, sulfuric acid is more readily accessible in substantial concentrations than hydrochloric acid (Al-Hussein, 2021). Furthermore, sulphuric acid does not produce chlorine gas or increase any chloride concentration in water, which may have negative effects on downstream processes (VITO, 2020). Regarding cost factors, sulfuric acid stands out as the singular potent acid that is typically more economical than hydrochloric acid. It holds the distinction of being the most affordable industrial acid on a global scale (Stephen, 2023).

In summary, H<sub>2</sub>SO<sub>4</sub> gains prominence in industrial applications due to its cost-effectiveness and effectiveness. However, it should be noted that chitosan's solubility behavior in both sulfuric acid and hydrochloric acid is

intricate, suggesting that complete dissolution might not occur. Consequently, further research and development are required to study the suitability of both acids for chitosan dissolution in the context of heavy metal removal.

## **2.5 Parameter Studies**

The heavy metal removal efficiency through the coagulation process can be influenced by various factors, including the initial concentration of metal ions, the quantity of coagulant used, the pH level of the solution, and the duration of contact. These are the parameters recognized to have an impact on the coagulation process and will be examined in this study.

### **2.5.1 Effect of Coagulant Dosage**

The amount of coagulant added to the wastewater has a significantly influences on the capacity to effectively remove heavy metal ions. Based on research from Pang, et al. (2009), the experimental results showed that the coagulant dosage would increase the removal efficiency of heavy metal and then declines due to excessive dosing. They found out that the removal of lead (II) ions by hydroxide precipitation increased only up to 98 % as the coagulant dosage increased to 1 g/L. The explanation provided was that the rise in the quantity of coagulant ions available to counteract the charges on heavy metals led to this phenomenon. Additionally, it was suggested that the escalation in heavy metal removal resulted in the increased collision of particles which was directly proportional to the coagulant dosage (Pang, et al., 2009).

However, it was pointed out that the excessive coagulant dosage can also have negative effects. While higher dosages might initially result in better charge neutralization and floc formation, overdosing can lead to excessive floc growth and coagulant wastage. Additionally, excessive floc size can hinder settling or flotation processes, reducing overall removal efficiency (Rosińska and Dąbrowska, 2021). Hence, the optimal coagulant dosage is crucial to achieve optimal heavy metal removal efficiency.

### 2.5.2 Effect of Solution pH

Out of all the factors, pH is the most important as it affects heavy metal removal efficiency in the coagulation process significantly. According to a study carried out by Huang, et al. (2020), it was found out that the optimum pH for removal of copper (Cu) by chitosan was around 6 – 7. The explanation provided clarified that when the pH is below 4, chitosan carries a positive charge due to protonation, causing it to repel copper ions. Conversely, at pH levels above 6, chitosan becomes deprotonated, resulting in a negative charge that attracts copper ions. Nonetheless, when pH reaches extremely high values beyond 8, copper undergoes hydroxide precipitation, limiting the availability of copper ions for chitosan adsorption (Huang, et al., 2020). Besides that, different coagulants work optimally within specific pH ranges. For instance, aluminum-based coagulants (like alum) are most effective in slightly acidic to neutral pH ranges, while ferric-based coagulants can work across a broader pH spectrum (Abdullah and Jaeel, 2019).

Furthermore, heavy metal ions in wastewater typically carries a charge. The degree of this charge is influenced by the solution pH values. As the pH changes, the charge on the heavy metal ions can change as well, affecting their interaction with coagulants (Alazaiza, et al., 2022). As an example, an experiment carried out by Bazrafshan, et al. (2015) showed that the optimum pH for removal of iron in wastewater by alum was found to be 6.5. Additional clarification was provided, indicating that when the pH is below 6, iron is predominantly present as soluble ferrous ions ( $\text{Fe}^{2+}$ ), which cannot be effectively precipitated by aluminum hydroxide. Conversely, when the pH exceeds 7, iron mainly takes the form of insoluble ferric ions ( $\text{Fe}^{3+}$ ), which competes with aluminum hydroxide for attachment points on the flocs (Bazrafshan, et al., 2015).

In summary, the pH of the solution is a crucial factor that impacts the effectiveness of heavy metal removal during the coagulation process. Selecting the appropriate coagulant and adjusting the pH within the recommended range for that coagulant are essential steps to achieve efficient heavy metals removal from wastewater.

### **2.5.3 Effect of Initial Heavy Metal Concentration**

The heavy metal removal efficiency can be influenced by the initial concentration of metal ions in wastewater. According to a study carried out by Tang, et al. (2016), a high coagulant dose was required in a low initial arsenate concentration (10  $\mu\text{g/L}$ ) to achieve a similar performance when compared to low coagulant dose in high initial arsenate concentration (500  $\mu\text{g/L}$ ) (Tang, et al., 2016). This was due to lesser chances for collisions between coagulant particles and metal ions, leading to the formation of few and low-density flocs. As a result, a significant amount of coagulant is needed to attain effective removal rates when dealing with low levels of metal ions.

An additional study conducted by Thakur, et al. (2021) demonstrated that as the initial concentration of lead increased from 10 to 100  $\text{mg/L}$ , the adsorption capacity of natural coagulant bentonite clay rose from 3.6 to 11.2  $\text{mg/g}$ . However, this capacity decreased to 9.9  $\text{mg/g}$  after surpassing 200  $\text{mg/L}$  of lead concentration (Thakur, et al., 2021). This indicates that there exists an ideal metal ions concentration range that can optimize the effectiveness of heavy metal removal using coagulation. When the concentration of metal ions becomes excessively high, there will no longer be vacant sites for adsorption on the coagulant.

## **2.6 Wastewater Sample Analysis**

It is crucial to understand the heavy metal removal efficiency with chitosan because it provides an understanding on how effective chitosan is in wastewater treatment. To understand the heavy metal removal efficiency of chitosan, various methods such as inductively coupled plasma optical emission spectroscopy (ICP-OES) can be used. It is an advanced analytical technique widely employed for both qualitative and quantitative analysis of elemental compositions across various sample types. It operates by utilizing a combination of plasma excitation and optical emission for analysis. In this method, when a wastewater sample is introduced into the torch of the instrument, it encounters a stream of argon gas, initiating a high-temperature plasma with temperatures surpassing 10,000  $^{\circ}\text{C}$ . This intense plasma environment serves to ionize and excite the heavy metal ions present in the sample, causing them to transition to higher energy states. As these ions are



disintegrated into their constituent atoms and return to their ground state, they emit light at distinct wavelengths characteristic of each element. Through gauging the intensity of these light at specific wavelengths, both the concentrations of heavy metals prior to and post coagulation can be determined (Sun, et al., 2019).

Scanning electron microscopy coupled with energy dispersive X-ray spectroscopy (SEM-EDX) is a method that merges an electron microscope with an X-ray detector to glean insights into a sample's structure and elemental makeup. When the coagulant after treating wastewater is exposed to an electron beam, it emits X-rays of distinct energies corresponding to the particular heavy metal it contains. By gauging the energy and strength of these X-rays, the presence of the heavy metal within the coagulants can be determined (Thermo Fisher Scientific Inc., 2023).

## **2.7 Oxidized Wastewater Treatment**

Some wastewater treatment sectors utilize aeration systems to oxygenate their wastewater, a process that can indirectly influence the coagulant dosage required for treatment. Research indicates that aeration can indirectly impact the amount of coagulant needed by oxidizing heavy metal ions, transforming them into less soluble states. For instance, manganese ions can undergo oxidation, leading to the creation of manganese dioxide ( $\text{MnO}_2$ ) particles. Consequently, oxidizing heavy metals prior to treatment may reduce the necessary coagulant dosage for achieving desired removal rates, as some heavy metals would already be partially precipitated (Jennifer, 2023).

The objective of this investigation is to assess the economic viability of treating oxidized wastewater compared to raw wastewater, as the required coagulant dosage for oxidized wastewater treatment may be lower which translates to cost savings (Shammas, et al., 2021).

## 2.8 Sludge Volume Index Study

The sludge volume index (SVI) is a parameter utilized in process control to depict the settling behavior of sludge within the aeration tank of an activated sludge process. SVI is computed to illustrate the tendency of activated sludge solids to thicken or concentrate during the sedimentation process (Ron, 2010). It also can be defined as the equation below:

$$\text{SVI (mL/g)} = \frac{\text{Settled Sludge Volume (mL/L)} \times 1000 \text{ mg/g}}{\text{Mixed Liquor Suspended Solids, MLSS (mg/L)}} \quad (2.6)$$

Next, it's crucial to understand the concept of mixed liquor suspended solids (MLSS). In wastewater treatment, mixed liquor denotes the amalgamation of either raw or unsettled wastewater, pre-settled wastewater, and activated sludge contained within an aeration tank (Saleha, 2023). MLSS primarily consists of microorganisms and non-biodegradable suspended matter. It has a crucial function in the activated sludge process by ensuring a sufficient quantity of active biomass is present to degrade organic pollutants effectively. This is frequently assessed using the food to microorganism ratio (F/M ratio). By sustaining an optimal F/M ratio, the biomass can effectively metabolize a large portion of the organic substances, thereby reducing the remaining food content in the treated effluent. Essentially, the more effectively the biomass metabolizes, the lower the biochemical oxygen demand (BOD) will be in the discharged water (Chemtech, 2020).

Effective MLSS management is vital for removing Chemical Oxygen Demand (COD) and BOD to purify water for various purposes, including surface water discharge and drinking water production. Raw sewage often contains concentrations of BOD reaching several hundred milligrams per liter (mg/L). By undergoing treatment procedures like screening, pre-settling, activated sludge treatment, or alternative methods, the BOD concentration in water can be significantly decreased to below 2 mg/L, fulfilling the standards for clean discharge or water recycling.

In summary, understanding SVI helps wastewater treatment plants optimize their processes and maintain efficient sludge settling.

## CHAPTER 3

### METHODOLOGY AND WORK PLAN

#### 3.1 Materials and Chemicals

The Table 3.1 below provides a list of the materials and chemicals utilized in the study. Both alum and chitosan will be used as the coagulants for removing heavy metal. The solution's pH values will be adjusted by using sulphuric acid, hydrochloric acid, and nitric acid. The heavy metal types present in the wastewater utilized for the parameter studies are also enumerated.

Table 3.1: List of Chemicals and Their Specifications.

<b>Chemical Reagent</b>	<b>Grade</b>	<b>Supplier</b>	<b>Usage</b>
Alum	Analysis	-	Chemical coagulant for removing heavy metal
Chitosan	87 % Purity	-	Natural coagulant for removing heavy metal
Hydrochloric Acid (HCl)	37 % Purity	-	Reagent for pH modification
Sulphuric Acid (H <sub>2</sub> SO <sub>4</sub> )	95 % Purity	-	Reagent for pH modification
Nitric Acid (HNO <sub>3</sub> )	65 % Purity	-	Reagent for pH modification
Nickel (Ni)	1000 mg/L	-	Model pollutant

The chemical characteristics, such as atomic weight and the wavelength of maximum absorption, will be used to investigate the removal of heavy metal efficiency are listed in Table 3.2.

Table 3.2: Chemical Properties of Heavy Metal Used in Research.

Heavy Metal	Symbol	Atomic Weight (amu)	Maximum Absorption Wavelength, $\lambda_{max}$ (nm)
Nickel	Ni	58.69	232

### 3.2 Equipment

The required instruments and equipment for this research are listed in Table 3.3, along with their brand/model and respective functions. To adjust the pH of the wastewater solution, a pH meter will be employed. An electric stopwatch will be utilized to document the contact time during the coagulation process. Analytical tools like ICP-OES, SEM-EDX, and FTIR spectrometer will be used for the characterization study. Lastly, a hot plate together with magnetic stirring bar will guarantee thorough mixing of the coagulant with the wastewater solution.

Table 3.3: Model and Functions of Instruments.

Instruments	Model	Function
Inductively Coupled Plasma Optical Emission spectroscopy	Optima 7000	Measurement of $\text{Ni}^{2+}$ in sample
Atomic Absorption Spectroscopy	Agilent 200 Series	Measurement of $\text{Ni}^{2+}$ in sample
Fourier Transform Infrared Spectrometer	Nicolet IS10	Analysis of coagulant compounds
Scanning Electron Microscope Energy Dispersive X-Ray	Hitachi S-3400 N	Morphology and elemental analysis
UV-Vis Spectrophotometer	Jenway 6320D	Measurement of treated water cleanliness
Hot Plate Magnetic Stirrer	IKA 362001 RET Basic	Mixing of coagulants in wastewater sample

### 3.3 Overall Flow of Study

The flowchart depicted in Figure 3.1 outlines the sequence of research activities. To commence, the coagulants, alum, and chitosan undergo a comprehensive characterization utilizing techniques like FTIR, SEM-EDX and XRD. Subsequently, the study progresses to parameter investigations. These involve altering the coagulant dosage, modulating the pH of the wastewater sample, and monitoring the initial nickel concentration to assess their effects on nickel removal efficiency. Furthermore, the research delves into exploring the impact of varying chitosan to alum ratios and the utilization of different acids for pH adjustment. Lastly, treatment for oxidized wastewater and examinations of the sludge volume index are conducted to gain deeper insights into the coagulation process.

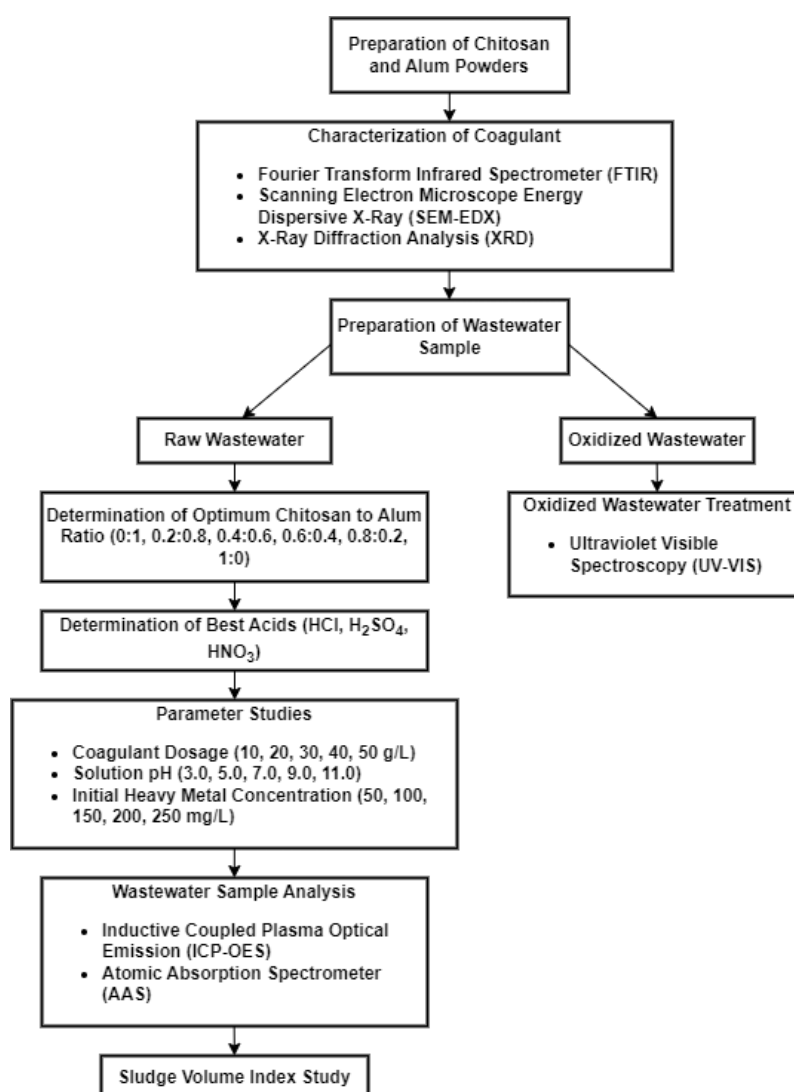


Figure 3.1: Overall Flow Diagram of Research.

### 3.4 Experimental Setup

Figure 3.2 illustrates the setup employed for the coagulation experiment. In this experimental setup, both the coagulants and wastewater were introduced into a beaker. To achieve thorough and uniform mixing of the coagulants with the wastewater sample, a hot plate and magnetic bar were employed.

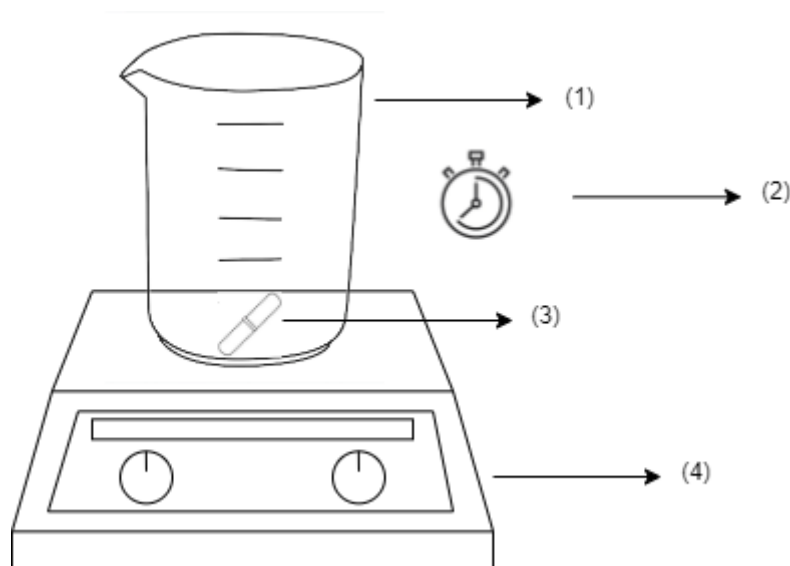


Figure 3.2: Diagrammatic Representation of the Experimental Setup (1) Beaker, (2) Stopwatch, (3) Magnetic Bar, (4) Hot Plate.

### 3.5 Experimental Procedures

#### 3.5.1 Preparation of Wastewater Sample

The wastewater samples, laden with Ni, are sourced from third-party suppliers to ensure consistency and reliability in the experimental setup. A volume of 1000 ml of wastewater, initially possessing a pH of 7.0, was carefully diluted to achieve a concentration of approximately 100 mg/L before commencing the experimental procedures.

#### 3.5.2 Preparation of Coagulant

Chitosan with an 87 % degree of deacetylation and 400 kDa molecular weight was supplied by QINGHEKANG Company. It exists as a white powder that readily dissolves in acids. To conduct the experiment, precisely 5 grams of chitosan was measured and carefully transferred into a 250 mL glass beaker. Following this, 25 ml of a 0.1 M HCl solution was introduced into the beaker

containing the chitosan, and the mixture will be left to stand for approximately 5 mins to aid in dissolution. Subsequently, the solution was subjected to stirring for an additional 5 mins at 250 rpm using a magnetic bar and hot plate. Further dilution of the solution was carried out by adding 125 mL of distilled water, and stirring was continued at an increased speed of 450 rpm until dissolution was achieved.

### **3.5.3 Characterization of Coagulants**

Characterization plays a pivotal role in comprehending the attributes of heavy metals and coagulants. It provides valuable insights into their composition, chemical structure, and chemical properties. Additionally, a thorough understanding of the coagulants' characteristics enables the evaluation of their performance. In this study, FTIR, SEM-EDX and XRD will be employed to characterize both heavy metals and coagulants.

FTIR was used to analyze the chemical compositions and structures of coagulants based on their interaction with infrared light. The model of the equipment that was going to be used was model Nicolet IS10. Next, SEM-EDX was used to ascertain the surface morphology and chemical composition of both the wastewater and coagulant samples. The process entails affixing the samples onto a pin stub, which is then placed inside a brass holder. The height of the sample is gauged in comparison to a reference height using provided measuring instruments, and the complete specimen dimensions are documented. The SEM is activated by initiating the beam, and the resulting image is observed and analyzed. Through the combined use of EDX with SEM, the chemical composition of the heavy metals and coagulants can be identified.

Finally, XRD analysis was employed to investigate various physical properties, including phase composition, crystal structure, and orientation, of both chitosan and alum powders.

### **3.6 Study of Different Chitosan to Alum Ratio for Nickel Removal**

A total of six coagulant solutions were prepared with different chitosan to alum ratio (0:1, 0.2:0.8, 0.4:0.6, 0.6:0.4, 0.8:0.2 and 1:0) to determine the optimum ratio for maximizing the nickel removal efficiency. The experiment was carried out with fixed parameters such as coagulant dosage of 40 g/L,

solution pH of 7 and initial nickel concentration of 100 mg/L. Firstly, 125 ml of wastewater sample was filled into a beaker together with coagulant of alum to chitosan ratio 0:1 under stirring. The beaker was stirred at 800 rpm for 6 minutes to disperse the coagulant solution. Next, the stirring speed was decreased to 200 rpm for 14 minutes to form the flocs. The stirrer was then switched off for 20 minutes for settling the flocs.

After the settling period, the sample was collected from the wastewater sample with a distance of 3 – 4 cm under the surface of beaker by syringe to ensure the accuracy of water quality assessments. The procedure was replicated for the remaining five sets, maintaining all other parameters at constant values. All experiments were carried out at room temperature. The samples were then analyzed using the ICP-OES. The optimum alum to chitosan ratio was utilized for the following parameter investigation.

### **3.7 Study of Different Acids for Nickel Removal**

After determining the optimum ratio for nickel removal efficiency, the effect of using different acids for adjusting pH as well as for dissolving coagulants was carried out. Initially, the coagulants, comprising one set with pure chitosan and another with the optimal chitosan to alum ratio, was precisely measured and deposited into separate glass beakers. Each of them was mixed with 25 mL of a 0.1 M HCl solution and left for approximately 5 minutes to facilitate dissolution. Subsequently, the solutions were subjected to stirring for an additional 5 minutes at 250 rpm using a magnetic bar and hot plate. Following this, the mixtures were each diluted with 125 ml of distilled water and stirred at 450 rpm until complete dissolution was achieved.

After carrying out the experiment aka coagulation, the process was repeated by replacing the HCl acid with H<sub>2</sub>SO<sub>4</sub> and HNO<sub>3</sub>. After the extraction of samples and subsequent centrifugation and filtration processes, the samples underwent another round of analysis. The most suitable acid for adjusting the pH was determined after conducting all the experiments.



### **3.8 Parameter Studies**

The efficiency of nickel removal through the coagulation process was investigated by altering operational variables, including the coagulant dosage (ranging from 10 to 50 g/L), solution pH (ranging from 3.0 to 11.0), and initial nickel concentration (ranging from 50 to 250 mg/L).

#### **3.8.1 Effect of Coagulant Dosage**

The impact of coagulant dosage on nickel removal efficiency was analyzed by varying the dosage from 10 to 50 g/L. Initially, 125 ml of wastewater sample was placed in a beaker with a coagulant dosage of 10 g/L. The solution temperature and pH were maintained at room temperature and 7.0, respectively. The stirring speed and duration was fixed for; (1) dispersing coagulant solution will be 800 rpm for 6 minutes, (2) formation of flocs was 200 rpm for 14 minutes, (3) settling period was 0 rpm for 20 minutes. After that, the sample was extracted by using syringe with a distance of 3 – 4 cm under the surface of beaker. The procedure was replicated for the remaining four coagulant dosages, maintaining all other parameters at constant values. Following the filtration and centrifugation processes, the samples underwent analysis using ICP-OES. The optimum coagulant dosage value was carried forward to be used in the following parameter studies.

#### **3.8.2 Effect of Solution pH**

The influence of solution pH on nickel removal efficiency was investigated by adjusting the pH to 3.0, 5.0, 7.0, 9.0, and 11.0. Firstly, 125 ml of wastewater sample at pH of 3.0 was filled into a beaker with optimum coagulant dosage. The temperature was fixed at room temperature. The stirring speed and duration was fixed for; (1) dispersing coagulant solution was 800 rpm for 6 minutes, (2) formation of flocs was 200 rpm for 14 minutes, (3) settling period was 0 rpm for 20 minutes. After that, the sample was extracted by using syringe with a distance of 3 – 4 cm under the surface of beaker. The procedure was then replicated for the remaining four pH values, maintaining the other parameters unchanged. Following the filtration and centrifugation processes, the samples underwent analysis using ICP-OES. The optimum pH value was carried forward to be used in the following parameter studies.

### 3.8.3 Effect of Initial Nickel Concentration

The effect of initial nickel concentration on the nickel removal efficiency was examined by setting the initial concentration at 50, 100, 150, 200 and 250 mg/L. Firstly, 125 ml of wastewater sample at 50 mg/L and at optimum pH was filled into a beaker with optimum coagulant dosage. The temperature was fixed at room temperature. The stirring speed and duration was fixed for; (1) dispersing coagulant solution was 800 rpm for 6 minutes, (2) formation of flocs was 200 rpm for 14 minutes, (3) settling period was 0 rpm for 20 minutes. After that, the sample was extracted by using syringe with a distance of 3 – 4 cm under the surface of beaker. The process was then repeated for the other 4 initial nickel concentrations while fixing the other parameters at constant value. Following the filtration and centrifugation processes, the samples underwent analysis using ICP-OES. The optimum initial nickel concentration was carried forward to be used in the following parameter studies.

### 3.9 Wastewater Sample Analysis

The wastewater samples collected from each experiment was subjected to analysis for nickel concentration using ICP-OES, specifically the Optima 7000 model. By quantifying the initial and final concentrations of nickel in the wastewater both before and after coagulation, the percentage of nickel removal efficiency can be calculated using the following equation:

$$\text{Nickel Removal Efficiency} = \frac{C_0 - C_f}{C_0} \times 100\% \quad (3.1)$$

where

$C_0$  = initial concentration of nickel, mg/L

$C_f$  = concentration of nickel after coagulation, mg/L

### 3.10 Oxidized Wastewater Treatment

A series of experiments will be conducted where oxidized wastewater will be treated with varying coagulant dosages (pure chitosan) of 10, 20, 30, 40, and 50 mg/L, while maintaining other optimum parameters established in previous studies. Additionally, the treated oxidized wastewater will undergo analysis

using UV-VIS spectroscopy to evaluate its cleanliness in comparison to distilled water.

### 3.11 Sludge Volume Index

To compute the sludge volume index (SVI), the sample must first undergo settling for a duration of 30 minutes before the analysis begins. Following this settling period, the volume of the settled sludge is observed and measured, typically expressed in milliliters per liter (mL/L).

To determine the mixed liquor suspended solids (MLSS) value, a filter paper must first be folded four times to form a cone shape. Subsequently, the filter paper should be placed in an oven and heated for thirty minutes. Following this, the filter paper should be weighed before being used for filtration with distilled water. The wastewater sample must be thoroughly mixed to ensure uniformity before pouring 50 mL of the sample onto the filter paper. Once filtration is complete, the filter paper should be placed back in the oven and heated at 100 °C for approximately 2h until completely dried. After drying, the final weight of the filter paper can be measured. Finally, the MLSS value can be calculated using the provided equation:

$$\text{MLSS} = \frac{(W_f - W_i) \times 1000 \times 1000}{\text{Volume of Sample (mL)}} \quad (3.2)$$

where

MLSS = mixed liquor suspended solids, mg/L

$W_f$  = final weight of filter paper, g

$W_i$  = initial weight of filter paper, g

Once the MLSS value has been determined, the SVI value can be calculated accordingly. With this, the settling characteristics of the sludge produced after coagulation process can be described.

## CHAPTER 4

### RESULTS AND DISCUSSION

#### 4.1 Characterization of Chitosan and Alum Powders

##### 4.1.1 FTIR Spectroscopy

Infrared spectroscopy is often used to identify both the organic and inorganic surface functional groups. Figure 4.1 below shows the FTIR spectrum of the pure chitosan used in this study. Functional groups that are crucial for nickel ion removal in chitosan, notably the hydroxyl (-OH) and amine (-NH<sub>2</sub>) groups were identified at characteristic wavenumbers of 3354 and 3286 cm<sup>-1</sup>, respectively.

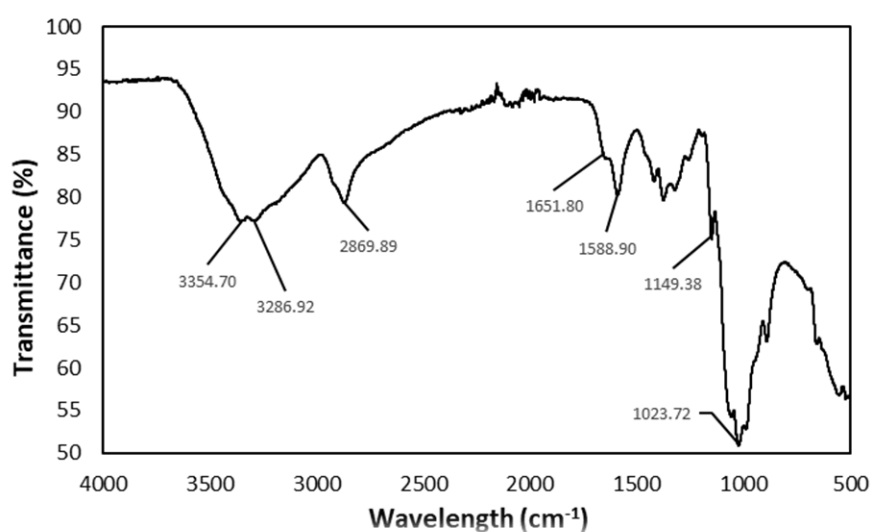


Figure 4.1: FTIR spectrum of pure chitosan.

In a study conducted by Nath et al. (2021), distinct absorption bands were observed in the FTIR spectrum of pure chitosan, particularly within the range of 3350 to 3450 cm<sup>-1</sup>, suggesting stretching vibrations linked to -OH group. Additionally, prominent peaks were evident between 3200 to 3400 cm<sup>-1</sup>, signifying the presence of reactive -NH<sub>2</sub> groups inherent in chitosan's molecular structure. Another noteworthy absorption band were observed around 1655 to 1630 cm<sup>-1</sup>, attributed to the C=O stretching of the amide I group. These functional groups, especially -OH and -NH<sub>2</sub> groups, are crucial

contributors to chitosan's capacity to bind metal ions effectively (Nath, Mishra and Pande, 2021).

As shown in Figure 4.2 below, when chitosan is dissolved in acids, it undergoes protonation, a process where hydrogen ions ( $H^+$ ) are added to the  $-NH_2$  groups. This protonation results in the formation of positively charged species ( $NH_3^+$ ) (Guibal, Vincent and Navarro, 2014). Consequently, the surface of chitosan, even when protonated, can adsorb nickel ions due to the presence of other functional groups such as  $-OH$  groups. These groups can interact with nickel ions and facilitate their adsorption onto the chitosan surface. Then, these nickel ions will replace the  $H^+$  ions on the amine groups through ion exchange and become bound to the chitosan matrix. Subsequently, the lone pair of electrons on the nitrogen atom in the amine group interacts with nickel ions, forming stable chelate complexes. These complexes prevent the nickel ions from remaining freely dissolved in water, effectively sequestering them within the chitosan matrix (Subbaiah and Sankaran, 2021).

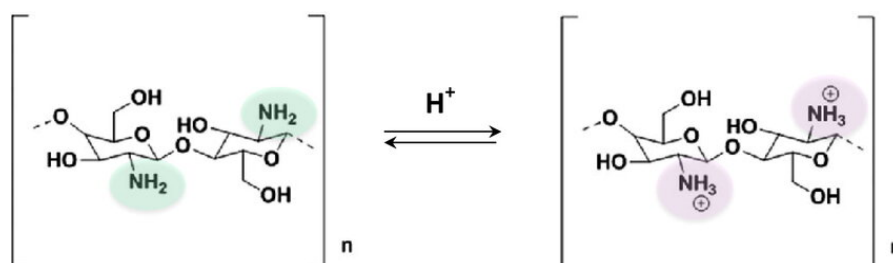


Figure 4.2: Protonation of the Amine Group in Chitosan (Yaneva, et al., 2020).

Once again, the spectrum obtained in Figure 4.1 closely aligns with previously reported findings in literature, confirming the presence of essential functional groups ( $-NH_2$  and  $-OH$ ) crucial for nickel ion removal. The fact that these functional groups were identified at the observed spectrum indicated that the purchased commercial chitosan was similar in terms of functional groups to those lab synthesized chitosan.

Figure 4.3 depicts the characteristic peaks identified in the spectrum of alum used in this study. Notably, the sulphate ( $-SO_4^{2-}$ ) group was located at  $923\text{ cm}^{-1}$ , the metal-oxygen (Al-O) bonds were evident at  $737\text{ cm}^{-1}$ , and the presence of  $-OH$  groups were observed at  $2931\text{ cm}^{-1}$ .

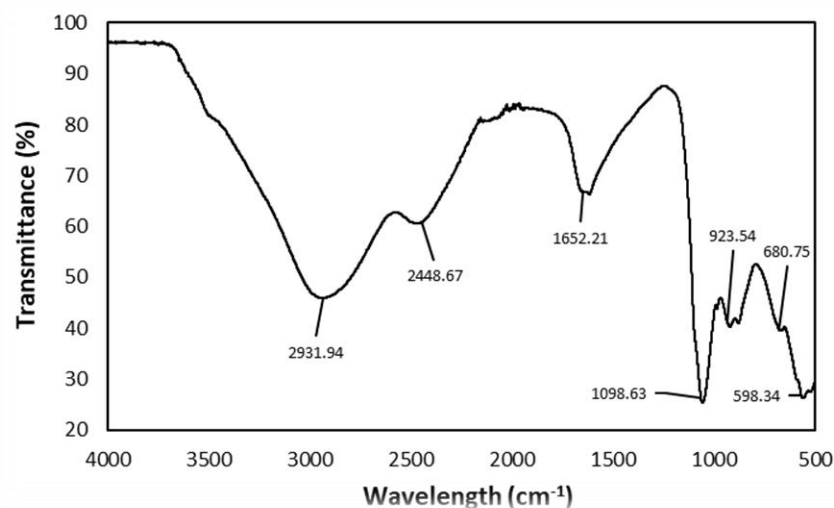


Figure 4.3: FTIR spectrum of alum.

In FTIR spectra of alum, distinct peaks are commonly identified, reflecting alum's structural components. The  $\text{-SO}_4^{2-}$  group is typically observed at between 900 and 1200  $\text{cm}^{-1}$ , indicative of stretching vibrations associated with S=O bonds. Additionally, peaks within the 400 to 750  $\text{cm}^{-1}$  range are attributed to the stretching of Al-O bonds inherent in alum. Furthermore, absorption bands spanning 2900 to 3500  $\text{cm}^{-1}$  signal the presence of -OH groups (Brandt et al., 2017). These groups also play an important role for the removal of nickel ions.

When alum is mixed with acids and water, it undergoes dissociation, releasing aluminum ions ( $\text{Al}^{3+}$ ) and sulfate ions ( $\text{SO}_4^{2-}$ ).  $\text{Al}^{3+}$  ions then react with water molecules to form hydroxide species, namely aluminum hydroxide,  $\text{Al}(\text{OH})_3$ . The presence of hydroxide groups within aluminum hydroxide leads to its overall negative charge, which in turn attracts and destabilizes the positively charged nickel ions present in the wastewater. As these nickel ions adhere to the surface of aluminum hydroxide, they form complexes. These complexes further aggregate, forming flocs. These flocs then function as nets, efficiently capturing and entrapping the metal ions within their structure as they precipitate out of the solution (Randive, et al., 2021).

The spectrum obtained in Figure 4.3 aligned closely with those documented in literature. This consistency confirmed the authenticity of the commercial alum utilized in this analysis.

#### 4.1.2 SEM-EDX

The surface morphology of the pure chitosan and pure alum were studied using SEM. As shown in Figure 4.4 (a), the SEM images of pure chitosan revealed a smooth, nonporous membranous structure with dome-shaped orifices, microfibrils, and crystallites (Abdullah Al Balushi et al., 2021). It appeared as interconnected networks or clusters due to their polymeric nature and ability to form complex structures. Based on Figure 4.4 (b), the general structure of alum consisted of elongated oval and irregular shapes characterized by uneven surfaces and edges. This irregular morphology was due to the crystalline arrangement of alum and the processes involved in its formation. Additionally, alum particles were seen to aggregate and form larger structures by adhering to each other due to attractive forces between alum molecules (Wijayati et al., 2021).

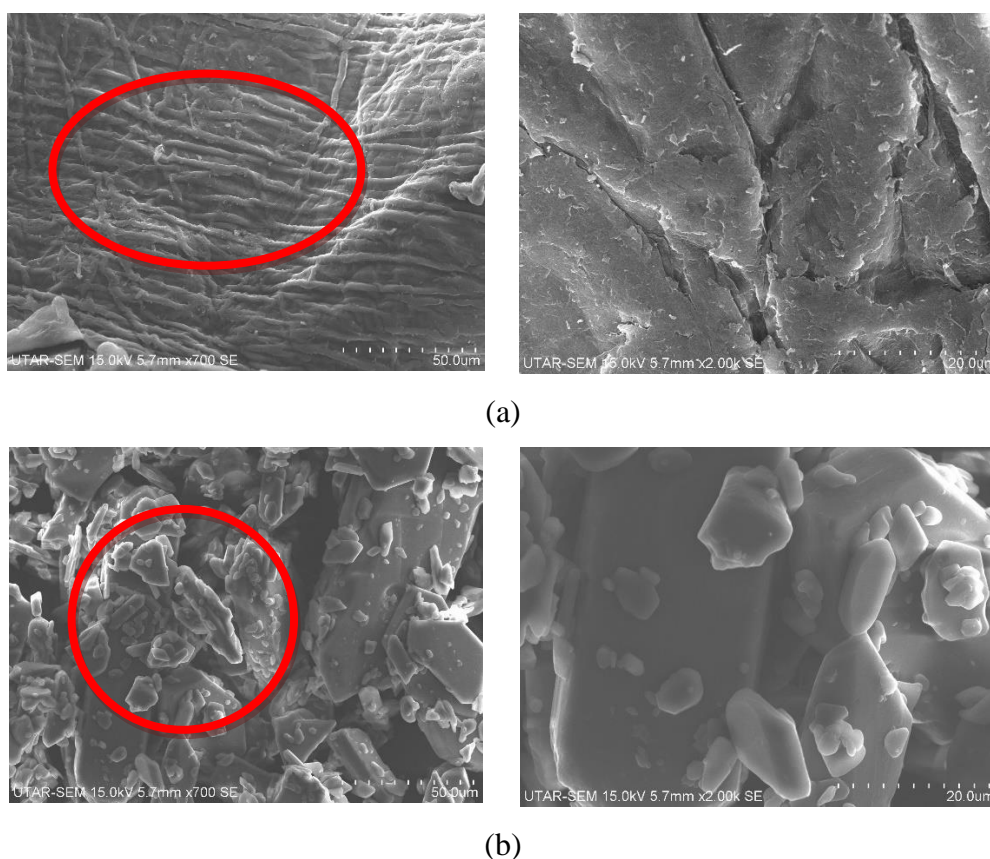


Figure 4.4: SEM Images of (a) Pure Chitosan and (b) Pure Alum.

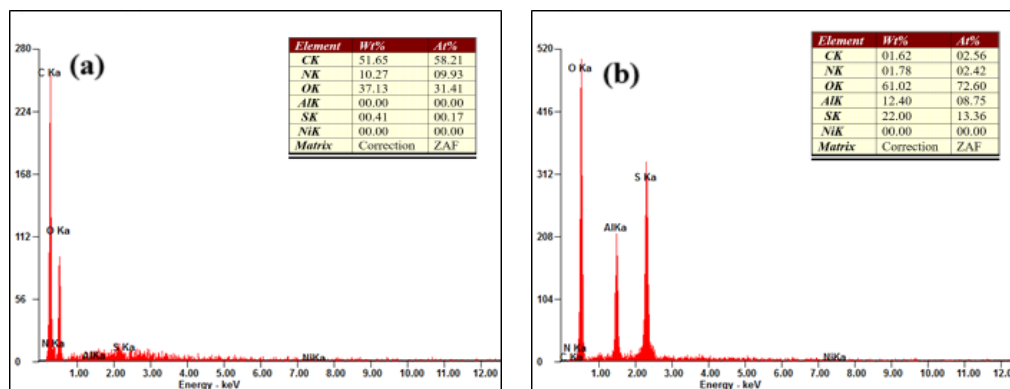


Figure 4.5: EDX Analysis for (a) Pure Chitosan and (b) Pure Alum.

Table 4.1: Distribution of Elements in Pure Chitosan and Pure Alum.

Sample	C (wt.%)	N (wt.%)	O (wt.%)	S (wt.%)	Al (wt.%)	Ni (wt.%)
Chitosan	51.65	10.27	37.13	0.41	-	-
Alum	1.62	1.78	61.02	22	12.40	-

The EDX analysis of chitosan alum and chitosan/alum composite was shown in Table 4.1. EDX analysis indicated that carbon (C), nitrogen (N), and oxygen (O) were the primary elements in chitosan. These elements are inherent to the chemical composition, reflecting the fundamental building blocks of chitosan. On the other hand, the analysis of alum showcased O, sulfur (S), and aluminum (Al) as the major constituents. These elements are integral to the sulfate ions and contribute to the overall composition of alum.



### 4.1.3 XRD

The X-ray diffraction (XRD) analysis was conducted on samples of pure chitosan and pure alum. The purpose was to examine their crystalline structures.

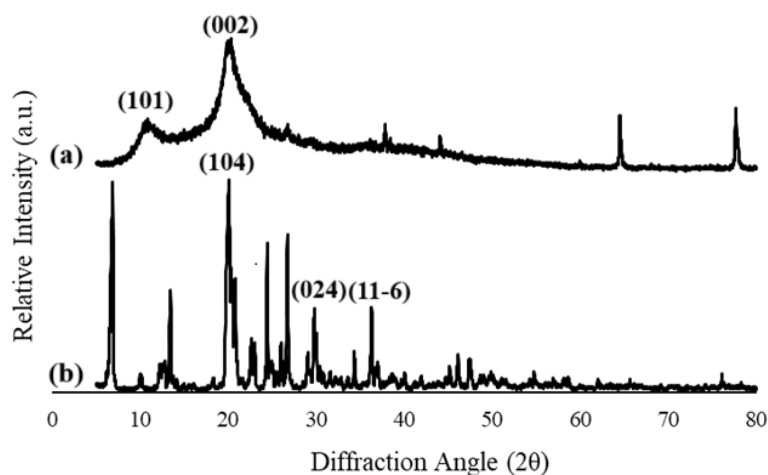


Figure 4.6: XRD Patterns for (a) Pure Chitosan and (b) Pure Alum.

The XRD patterns for pure chitosan as depicted in Figure 4.6 (a) revealed broad peaks centered at approximately  $2\theta = 10^\circ$  and  $20^\circ$ , corresponding to the (101) and (002) crystallographic planes, respectively. Additionally, the characteristic peaks at  $2\theta$  values of  $10.9^\circ$  and  $19.8^\circ$ , indicated the amorphous structure of chitosan (Purohit and Rawat, 2022). The crystal lattice of chitosan includes both crystalline and amorphous domains. The crystalline regions contribute to chitosan's mechanical strength, providing structural integrity, while the amorphous regions enhance its flexibility and solubility, allowing for versatility in applications (Julkapli, Ahmad and Akil, 2010).

Figure 4.6 (b) depicts the crystallinity and crystal lattice of alum with peaks at  $2\theta = 20.48^\circ$  (104),  $24.4^\circ$  (11-3),  $29.77^\circ$  (024) and  $36.3^\circ$  (11-6). These peaks shows that alum adopts a face-centered cubic (FCC) cubic structure where the atoms are arranged in a three-layer sequence, resulting in a dense geometric packing.

#### 4.2 Study of Different Chitosan to Alum Ratio for Nickel Removal

The effect of chitosan to alum ratio on the removal efficiency of nickel ions in wastewater was carried out which with range between 0:1 to 1:0. This study aims to evaluate the efficacy of chitosan as either a standalone coagulant or a coagulant aid in wastewater treatment. By identifying the most efficient ratio, it seeks to optimize the utilization of chemicals such as alum, thereby potentially reducing costs and minimizing associated risks (Takaara and Kurumada, 2023).

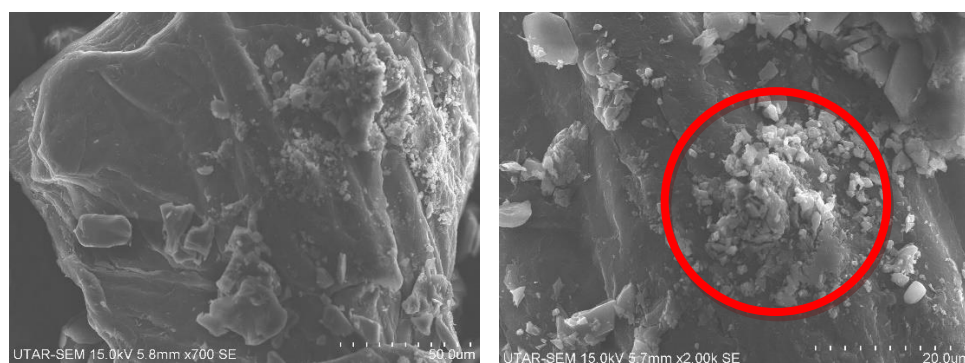


Figure 4.7: SEM Images of Chitosan/Alum Composite.

Based on the Figure 4.7, the morphology of the chitosan/alum composite revealed that the alum particles had adhered to the surface of the chitosan. Moreover, the surfaces of the composite exhibited rougher textures, with micro-cracks and irregular features when compared to the smooth surfaces shown in pure chitosan (Figure 4.4 (a)). This could be due to the result from particle interactions, surface oxidation, or surface modifications during the handling of composite (Mohamed, et al., 2009).

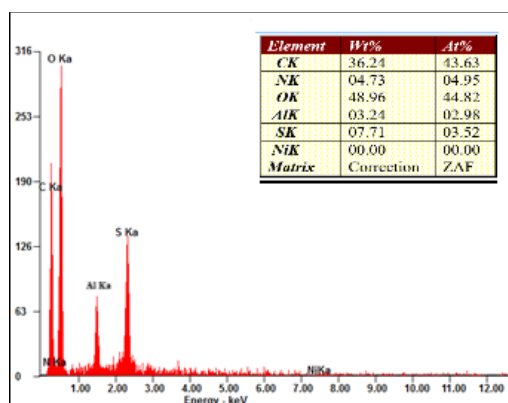


Figure 4.8: EDX Analysis for Chitosan/Alum Composite.

Table 4.2: Distribution of Elements in Chitosan/Alum Composite.

Sample	C (wt.%)	N (wt.%)	O (wt.%)	S (wt.%)	Al (wt.%)	Ni (wt.%)
Chitosan/Alum = 0.4:0.6	36.24	4.73	48.96	6.71	3.24	-

Based on the Table 4.2, the weight percentage of each element in the chitosan/alum composite fell within the range observed in both pure chitosan and pure alum, as indicated in Table 4.1. This suggests that chitosan and alum particles were effectively mixed and dispersed within the composite material.

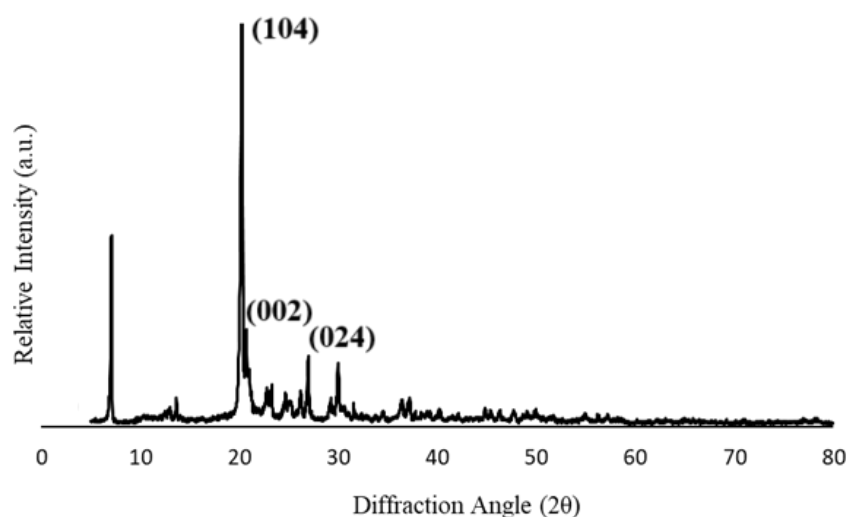


Figure 4.9: XRD Patterns for Chitosan/Alum Composite (0.4:0.6).

For the chitosan/alum composite shown in Figure 4.9, the diffraction peaks observed were close to those detected in the XRD patterns of pure chitosan and alum shown in Figure 4.6. It can be observed that the number of average peak intensity were reduced when compared to the ones in pure chitosan and alum. Hence, this proved that combining both chitosan and alum had helped in limiting the peaks corresponding to their individual counterparts.

Figure 4.10 shows the effect of chitosan to alum ratio to the removal efficiency of Ni ions.

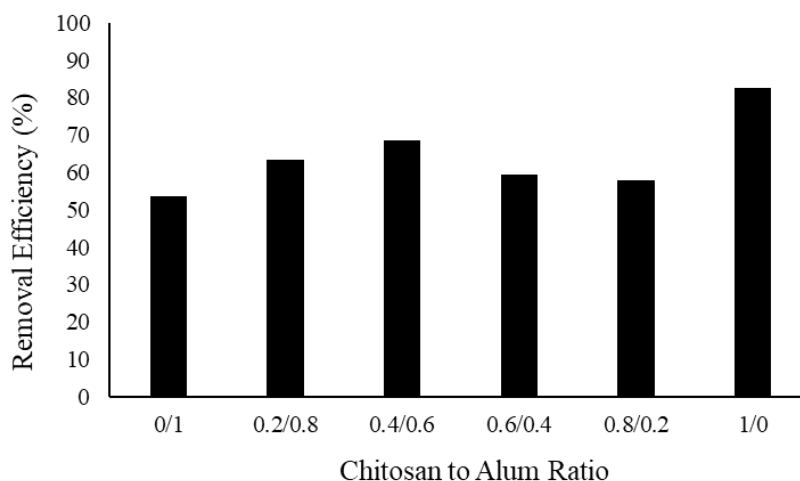


Figure 4.10: Effect of Chitosan to Alum Ratio on the Nickel Removal (Coagulant Dosage = 40 g/L, Initial Ni Concentration = 100 mg/L, pH = 7, Contact Time = 20 minutes, Acid Type = HCl).

As the chitosan to alum ratio rised from 0:1 to 0.4:0.6, there was a noticeable increase in removal efficiency. According to Tahraoui, et al. (2024), pure alum in water treatment often requires the addition of flocculants to maximize its efficiency. While alum aids in the destabilization of particles in water, the introduction of flocculants enhances the aggregation of these destabilized particles into larger flocs. As no additional flocculants were introduced during this study, it is understandable that pure alum exhibited the lowest removal efficiency compared to other treatments (Tahraoui, et al., 2024).

When the ratio was increased to 0.4:0.6, the removal efficiency reached its peak, indicating an optimal balance between chitosan and alum. However, as the ratio further increased, the removal efficiency began to decrease slightly. One possible explanation for this phenomenon could be due to the potential binding of aluminum ions by excess chitosan. In such cases, the aluminum ions released by alum may bind to chitosan, reducing the available binding sites for both chitosan and alum (Machado, Esteves and Pires, 2024). Another possible explanation could be due to the buffering effect possessed by excess chitosan, altering the ionic strength of the wastewater, potentially influencing the solubility and hydrolysis of alum (Pinotti, Bevilacqua and Zaritzky, 1999). Considering these observations, it was

determined that pure chitosan would be more suitable for further investigations as a standalone coagulant.

### 4.3 Study of Different Acids for Nickel Removal

The effect of different types of acids on dissolving coagulants and adjusting wastewater pH for nickel removal efficiency was investigated. Three acids were utilized in the study: HCl, H<sub>2</sub>SO<sub>4</sub>, and HNO<sub>3</sub>. As depicted in Figure 4.11, it was evident that H<sub>2</sub>SO<sub>4</sub> yielded the most favorable results, with a removal efficiency of 96.13 % for pure chitosan and 60.2 % for the chitosan/alum composite with a ratio of 0.4:0.6. Following H<sub>2</sub>SO<sub>4</sub>, HCl exhibited a removal efficiency of 80.38 % and 55.22 %, while HNO<sub>3</sub> demonstrated a removal rate of 78.46 % and 54.73 %, for pure chitosan and chitosan/alum composite with a ratio of 0.4:0.6, respectively. Once more, it was confirmed that pure chitosan exhibited superior removal efficiency compared to using chitosan as a coagulant aid.

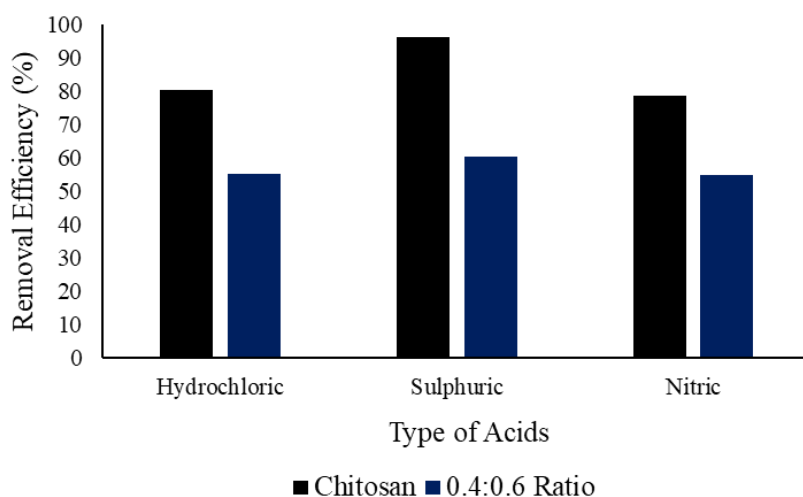


Figure 4.11: Effect of Type of Acids on the Nickel Removal (Coagulant Dosage = 40 g/L, Initial Ni Concentration = 100 mg/L, pH = 7, Contact Time = 20 minutes).

In the case of H<sub>2</sub>SO<sub>4</sub>, it acted as a diprotic acid, capable of donating two H<sup>+</sup> ions per molecule. This characteristic enabled it to dissolve twice as much per concentration compared to HCl or HNO<sub>3</sub> (Sajid, 2023). With this advantage, H<sub>2</sub>SO<sub>4</sub> exhibited a higher capacity to protonate the amino groups

present in chitosan molecules, resulting in faster and more complete dissolution of chitosan. Moreover,  $\text{H}_2\text{SO}_4$  provided a more stable environment for chitosan dissolution when compared to  $\text{HCl}$  or  $\text{HNO}_3$ . Conversely, among the three acids,  $\text{HNO}_3$  yielded the least favorable results due to its weaker potency compared to the other two. Consequently, it was less effective in dissolving the coagulants, resulting in lower removal efficiency. Based on the findings of the study, it is evident that  $\text{H}_2\text{SO}_4$  is the superior choice for dissolving coagulants, both in terms of effectiveness and cost-effectiveness (Al-Hussein, 2021).

#### 4.4 Parameter Studies

##### 4.4.1 Effect of Chitosan Dosage

The effect of chitosan dosage on the removal of heavy metal in wastewater was carried out with initial Ni concentration of 100 mg/L and pH of 7.0. Figure 4.12 shows the Ni removal efficiency with various chitosan dosage (in the range of 10 to 50 g/L).

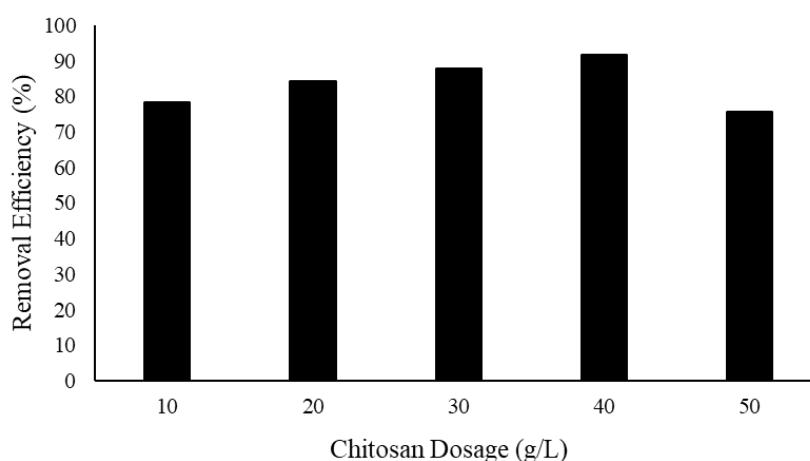


Figure 4.12: Effect of Chitosan Dosage on the Nickel Removal (Initial Ni Concentration = 100 mg/L, pH = 7, Contact Time = 20 minutes, Acid Type =  $\text{H}_2\text{SO}_4$ ).

As shown in Figure 4.12, the Ni removal efficiency increased steadily when the chitosan dosage increased from 10 g/L to 40 g/L. This phenomenon may be attributed to the increased surface area available for Ni ions to adhere to. This amplifies the likelihood of interaction between the chitosan and the Ni

ions, consequently enhancing the adsorption process (Wang et al., 2021). Moreover, an elevated dosage of chitosan offered an increased number of active sites characterized by  $-NH_2$  and  $-OH$  groups, facilitating the binding of Ni ions. As per research findings, it was noted that chitosan exhibits a buffering effect on the solution's pH. This attribute proves advantageous for maintaining the stability of the complexes formed between nickel and chitosan during the coagulation process (Zhang, Zeng and Cheng, 2016). Therefore, it is proposed that the increased collision of particles also led to an enhanced removal of Ni ions, which exhibited a proportional relationship with the chitosan dosage up to a specific threshold (Pang, et al., 2009).

Nevertheless, at a chitosan dosage of 50 g/L, there was a noticeable decline in the removal efficiency. This could be attributed to the saturation of excessive chitosan, thereby diminishing the coagulation process between the coagulants and the heavy metals. Consequently, a chitosan dosage of 40 g/L was selected for further investigations into the parameters.

#### 4.4.2 Effect of Solution pH

The effect of solution pH on the removal of heavy metal in wastewater was carried out in the range of pH of 3 to pH 11, tuning with 1M  $H_2SO_4$  or 1M NaOH. Figure 4.13 shows effect of solution pH to Ni removal efficiency.

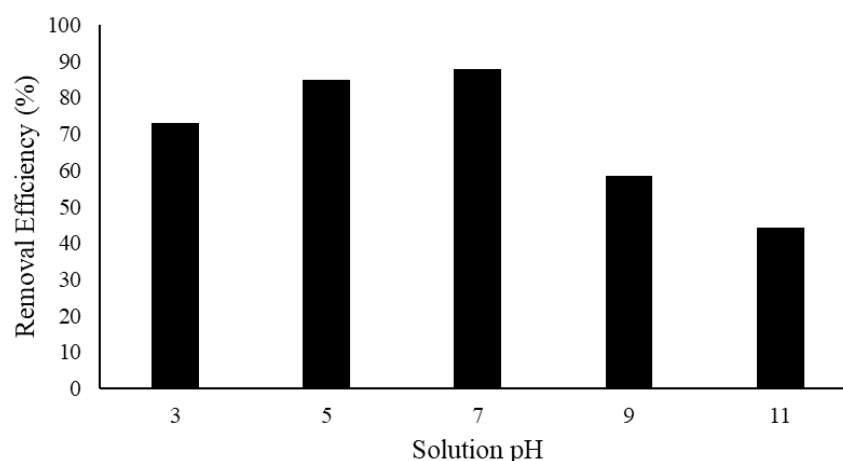


Figure 4.13: Effect of Solution pH on the Nickel Removal (Chitosan Dosage = 40 g/L, Initial Ni Concentration = 100 mg/L, Contact Time = 20 minutes, Acid Type =  $H_2SO_4$ ).

It could be observed that as the solution pH increased from 3 to 7, there was a noticeable increase in removal efficiency. Such observation was in agreement with those reported in literatures. According to Huang et al. (2020), at pH below 4, the  $\text{-NH}_2$  groups in chitosan underwent excessive protonation, which eventually led to repulsion of positively charged metal ions and a reduction in the coagulation rate. Another potential reason could be attributed to the exceptionally high solubility of chitosan in low pH, which hindered its interaction with Ni ions by keeping the chitosan in solution instead of forming flocs (Xu et al., 2021). Additionally, the elevated concentration of  $\text{H}^+$  ions at lower pH levels could compete with Ni ions for binding sites on chitosan, reducing its ability to capture Ni ions effectively. Consequently, solutions with low pH were found to be unfavorable for the coagulation process of Ni ions.

On the other hand, when the pH exceeded 5, the protonation level and solubility of chitosan reached an optimal state. Additionally, the Ni-chitosan complexes formed were most stable at nearly neutral pH, effectively preventing the release of Ni ions back into the solution (Rahman et al., 2023). However, as depicted in Figure 4.13, when the pH surpassed 7, there was a significant decrease in the removal efficiency. This occurrence was due to the precipitation of Ni ions as nickel hydroxide ( $\text{Ni(OH)}_2$ ), reducing their availability for chitosan adsorption (Huang, et al., 2020). At higher pH levels, the deprotonation of  $\text{-NH}_2$  groups may occur, causing structural alterations in chitosan. These changes could potentially impact its capability to create complexes with Ni ions. Therefore, considering the findings of the study, a solution pH of 7 was chosen as the optimal condition for the subsequent parameter investigations.

#### **4.4.3 Effect of Initial Nickel Concentration**

The effect of initial Ni concentration on the removal efficiency of Ni ions in the wastewater was carried out in the range between 50 to 250 mg/L. Figure 4.14 shows the removal efficiency of Ni ions in different initial Ni concentration.



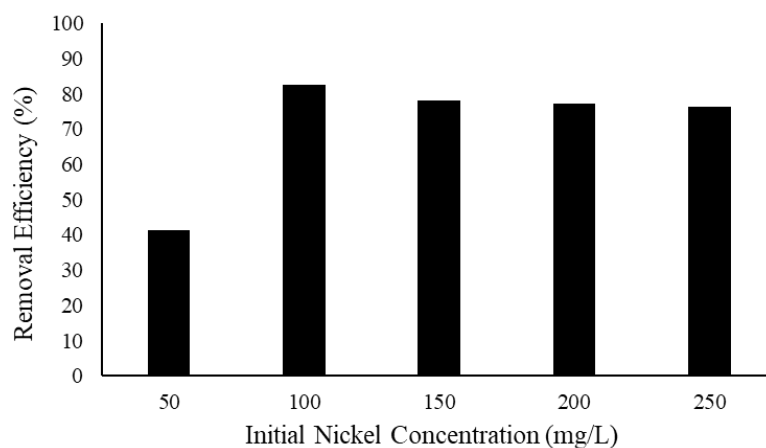


Figure 4.14: Effect of Initial Nickel Concentration on the Nickel Removal (Chitosan Dosage = 40 g/L, pH = 7, Contact Time = 20 minutes, Acid Type = H<sub>2</sub>SO<sub>4</sub>).

At an initial concentration of 50 mg/L, the removal efficiency was notably low. This was attributed to the limited opportunities for collisions between chitosan particles and Ni ions in a fixed mixing duration, resulting in the formation of few and low-density flocs. Additionally, in wastewater containing 50 mg/L of Ni ions, the volume of water is greater compared to the quantity of Ni present. This dilution effect can diminish the overall effectiveness of the coagulation process because the Ni concentration per unit volume of water is lower, leading to a decreased availability of Ni ions for removal. As a result, to overcome the decreased chance of collision and achieve effective removal rates at lower concentrations of Ni ions, a greater quantity of chitosan may be necessary (Thakur, et al., 2021). As the initial concentration increased to 100 mg/L, a significant increase in the removal efficiency of Ni ions was observed. However, the efficiency gradually decreased after surpassing a Ni concentration of 100 mg/L. When the concentration of metal ions was in excess, the coagulation efficiency would drop as the coagulant was saturated with Ni ions. Based on the results of the study, an initial nickel concentration of 100 mg/L was selected as the optimal condition.

#### 4.5 Characterization of Chitosan Sludge

To confirm the effectiveness of the coagulation process, the chitosan sludge obtained after treating the wastewater was processed into powder form through heating and drying. Figure 4.15 belows compare the physical appearance of chitosan powder before and after treating the wastewater.

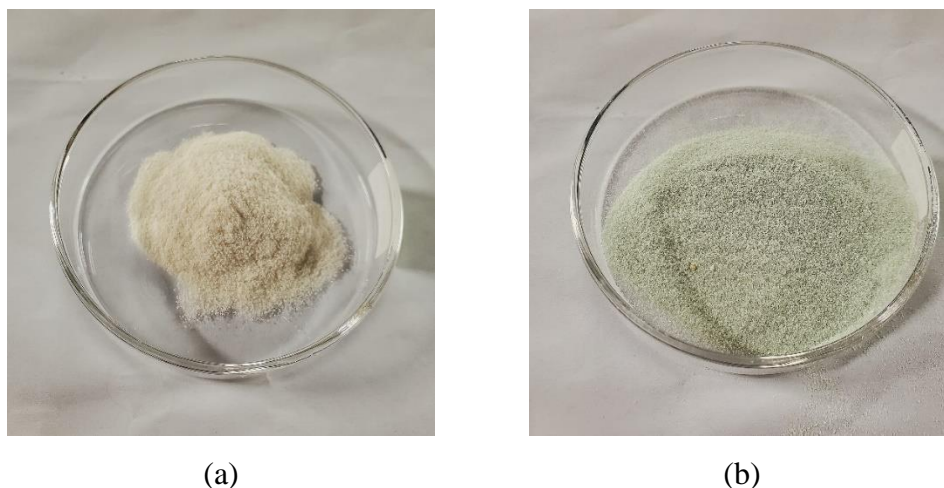


Figure 4.15: Comparison of Chitosan Powder (a) Before and (b) After Treatment.

As depicted in Figure 4.15 (a), the chitosan powder initially exhibited a white, translucent appearance. Following its application in wastewater treatment, the chitosan sludge underwent a process of heating and drying, returning it to a powder form. The resulting powder displayed a green hue, as depicted in Figure 4.15 (b). This demonstrated the successful removal of Ni ions from wastewater by the chitosan powder. Subsequently, the chitosan sludge powder underwent analysis using SEM-EDX for further validation.

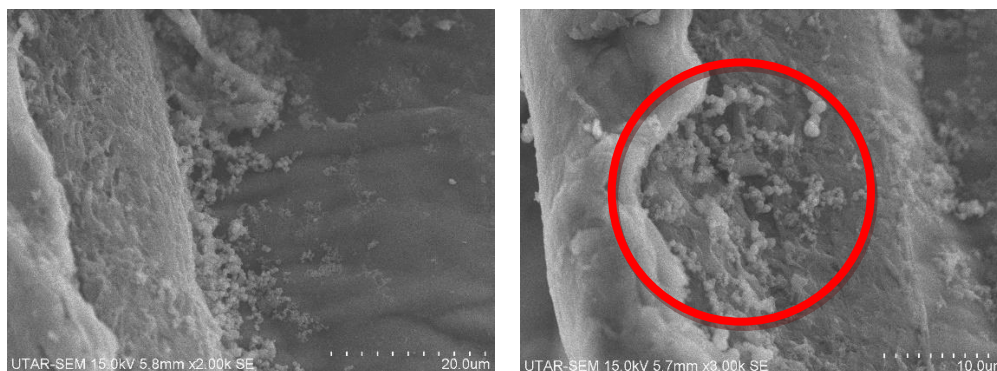


Figure 4.16: SEM Images of Chitosan Sludge at Different Magnification.

Based on the Figure 4.16, the SEM images taken at magnifications of 2000x and 3000x displayed microscopic granular particles that were closely attached to the surface of the chitosan. This phenomenon was not observed on the surface of pure chitosan. (Figure 4.4 (a)). These particles were nickel particles and appeared as spherical structures with a dotted-like appearance. Additionally, the nickel particles were observed to agglomerate or cluster together due to attractive forces between each individual particles (Murtaza, et al., 2023).

Table 4.3: Distribution of Elements in Chitosan Sludge.

<b>Sample</b>	<b>C</b> <b>(wt.%)</b>	<b>N</b> <b>(wt.%)</b>	<b>O</b> <b>(wt.%)</b>	<b>S</b> <b>(wt.%)</b>	<b>Al</b> <b>(wt.%)</b>	<b>Ni</b> <b>(wt.%)</b>
Chitosan Sludge	47.32	5.17	35.58	3.38	-	8.55

As indicated in Table 4.3, the chitosan sludge contained nickel elements, with a weight percentage of 8.55 %, whereas pure chitosan, as shown in Table 4.1 did not exhibit any nickel presence. This clearly indicated that chitosan effectively entrapped nickel ions in the wastewater, aiding in heavy metal removal.

#### 4.6 Oxidized Wastewater Treatment

The impact of varying chitosan dosages on the removal of heavy metal oxides in oxidized wastewater was investigated. Figure 4.17 depict the raw wastewater and oxidized wastewater both before and after treatment, including images taken prior to treatment and after the settling process.

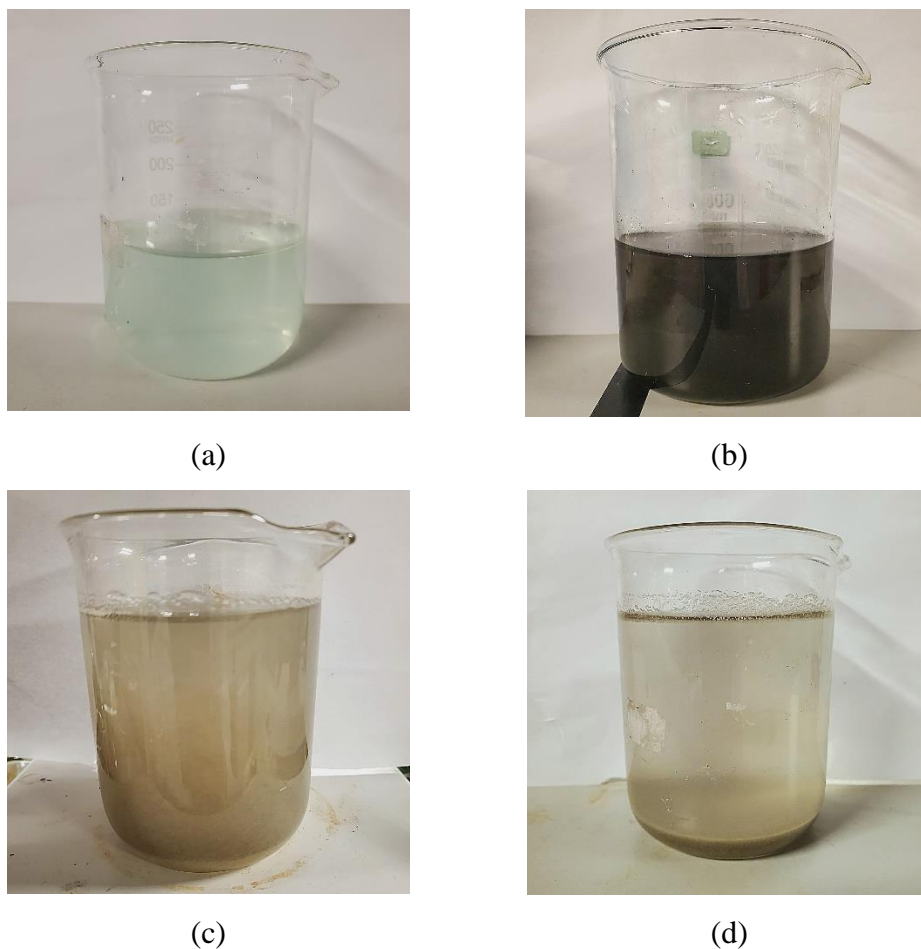


Figure 4.17: Images of (a) Wastewater; (b) Oxidized Wastewater; (c) Treated Wastewater Before Settling and (d) Treated Wastewater After Settling for 30 minutes.

It was evident from Figure 4.17 (b) that the oxidized wastewater exhibited a dark coloration as compared to the original raw wastewater that exhibited light green colour in Figure 4.17 (a) after two weeks of air exposure. This attributed to the oxidation of Ni ions in the wastewater. The dark particles in the wastewater was recovered by centrifugation process and then subjected for XRD analysis.

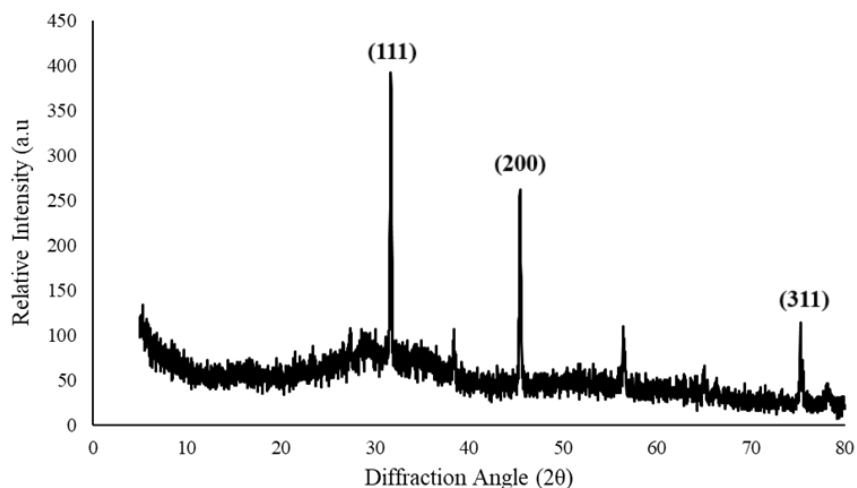


Figure 4.18: XRD Patterns for Oxidized Wastewater.

Figure 4.18 illustrates the XRD patterns specifically for nickel oxide (NiO), revealing distinct peaks observed at  $2\theta = 32^\circ$ ,  $44^\circ$ , and  $75^\circ$ . These peaks correspond to the crystallographic planes of (111), (200), and (311) respectively, indicative of the face-centered cubic (fcc) crystal structure characteristic of NiO (A. F. Lahiji, et al., 2023).

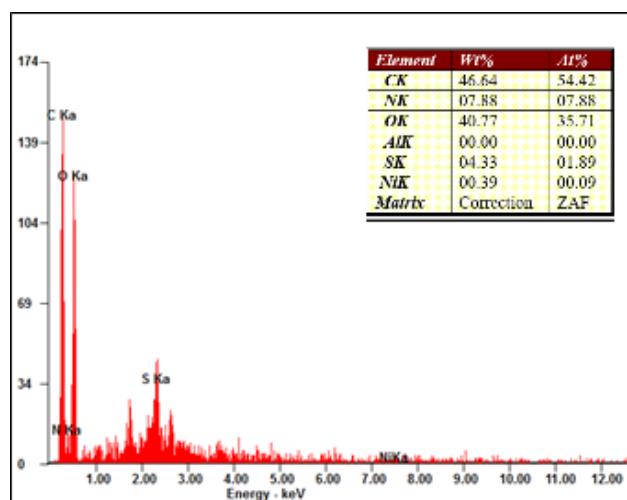


Figure 4.19: EDX Analysis for Oxidized Sludge.

Table 4.4: Distribution of Elements in Oxidized Sludge.

Sample	C (wt.%)	N (wt.%)	O (wt.%)	S (wt.%)	Al (wt.%)	Ni (wt.%)
Oxidized Sludge	46.64	7.88	40.77	4.33	-	0.39

Based on the Table 4.4 , the weight percentage of oxygen element were found to be higher than in normal sludge (Table 4.3). This indicated that more oxygen had combined with nickel to create nickel oxides within the sample.

Based on the Figure 4.17 (c) After the oxidized wastewater went through the coagulation process, it was evident that the color of the oxidized wastewater has noticeably lightened compared to its before treatment state. Upon allowing it to settle for 30 min, the solution reveals distinct layers of color. The upper portion of the sample appears significantly clearer than before treatment, while the sediment, or sludge, generated during the process has settled at the bottom of the container. This clearly demonstrated that the coagulation process has effectively eliminated or captured the majority of the contaminants present in the wastewater.

To further confirm that the oxidation process had successfully reduced the concentration of Ni ions in the wastewater, four samples obtained after centrifugation underwent analysis using ICP-OES and the results are shown in Table 4.5 below.

Table 4.5: ICP-OES Analysis of Nickel Ions in Oxidized Wastewater.

<b>Sample</b>	<b>Concentration of Ni<sup>2+</sup> (mg/L)</b>
a	0.00
b	0.00
c	0.00
d	0.00

Table 4.5 shows that that the concentration of nickel in all four samples of oxidized wastewater was measured at 0 mg/L. This clearly demonstrates the complete oxidation of nickel ions into nickel oxides.

For the treatment of oxidized wastewater, different coagulant dosages ranging from 10 to 50 g/L were examined. A UV-VIS double beam spectrophotometer was employed to investigate the purity of treated wastewater in comparison to oxidized wastewater, specifically at a wavelength of 240 nm. The treated wastewater was expected to exhibit a decrease in absorbance value, indicating higher transparency and a lower concentration of

contaminants present in the sample. By analyzing the absorbance peak obtained for both the oxidized wastewater and treated wastewater, the removal efficiency was computed and shown in Figure 4.20 below.

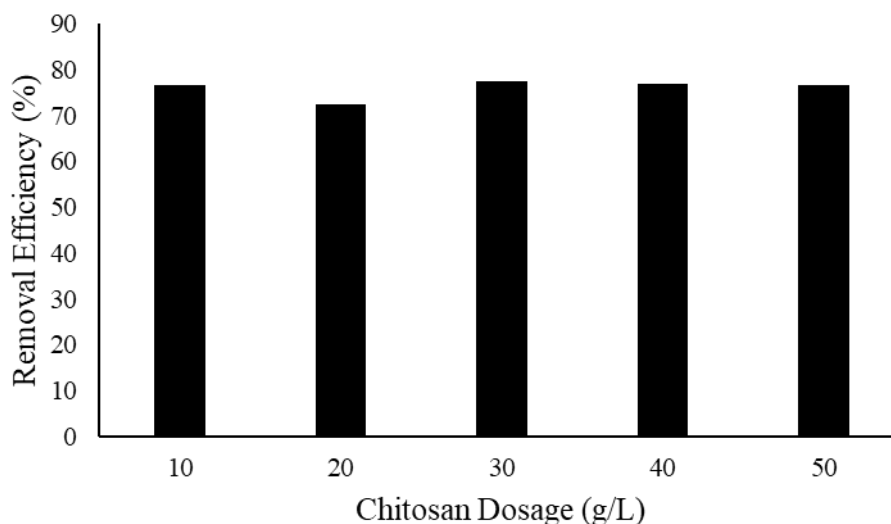


Figure 4.20: Effect of Chitosan Dosage on the Removal of Nickel Oxide.

Based on the Figure 4.20, the optimal chitosan dosage of 30 g/L was identified, as it exhibited the highest removal efficiency. The optimal dosage of chitosan for treating oxidized wastewater was found to be lower than that required for treating raw wastewater. This reduction could be attributed to several factors, one of which is the promotion of larger and more easily removable particles in the wastewater facilitated by the oxidation process (Saritha, Srinivas and Srikanth Vuppala, 2017). Additionally, oxidation has the effect of breaking down complex organic compounds, thereby decreasing their ability to interfere with the coagulation process.

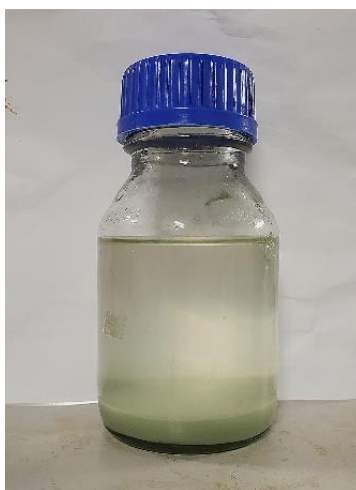
Nevertheless, considering that the increase in removal efficiency from 10 g/L to 30 g/L was only 0.8447 %, it is advisable to stick with a chitosan dosage of 10 g/L for treating oxidized wastewater. This is because a lower coagulant dosage while achieving effective removal translates to cost savings in terms of supplying, handling and disposal.

#### 4.7 Sludge Volume Index Study

As previously discussed, the Sludge Volume Index (SVI) serves as a process control parameter, indicating the settling characteristics of sludge in the tank containing sludges. Conversely, Mixed Liquor Suspended Solids (MLSS) is another critical parameter that warrants attention to mitigate process disruptions and maintain treatment reliability. Managing SVI and MLSS effectively is indispensable for efficient wastewater treatment operations.

According to the Figure 4.21, the treated wastewater underwent a settling period of 30 mins. After the settling period, the volume of sludge observed and measured was 26 mL per 250 mL of the treated wastewater. Consequently, after computation, the resulting final value obtained was 104 mL/L. This finding indicates that for every liter of treated wastewater, the wet volume of settled sludge is approximately 104 mL.

To measure the MLSS concentration, an initial filter paper weight of 0.5103 grams was recorded, and a 50 mL sample was filtered. Subsequently, the filtered sample underwent heating in an oven at 100 °C for a duration of 2 hours. After this process, the final filter paper weight was measured and found to be 0.9109 grams. Table 4.6 provides a comprehensive overview of the results obtained from the Sludge Volume Index calculation, incorporating the initial and final filter paper weights, the volume of the sample filtered, and the corresponding MLSS concentration.



(a)

Figure 4.21: Treated Wastewater Sample Used for SVI Study.



Table 4.6: Summary of SVI Calculation.

<b>Parameter</b>	<b>Value</b>
Settled sludge volume	104 mL/L
Initial filter paper weight, $M_0$	0.5103 g
Final filter paper weight, $M_1$	0.9109 g
Volume of filtered sample, $V$	50 mL
<b>Mixed liquor suspended solids, MLSS</b>	<b>8012 mg/L</b>
<b>Sludge volume index, SVI</b>	<b>12.98 mL/g</b>

According to the Table 4.6, the determined MLSS value of 8,012 mg/L has exceeded the typical concentration range of MLSS, which was generally observed to be between 1,500 mg/L to 5,000 mg/L in conventional wastewater treatment plants (Saleha, 2023). According to a research by Kevin. (2022), high flow rates or inadequate settling times can contribute to higher MLSS values within a wastewater treatment system. These conditions may lead to the formation of a thick sludge blanket, which can indirectly impact effluent quality by impeding proper treatment processes (Kevin, 2022).

It is important to highlight that the treated wastewater utilized in this study was not subjected to any tertiary treatment or filtration. As a result, the recorded MLSS value may not precisely reflect what would be observed in an actual wastewater treatment facility. In practical wastewater treatment settings, lowering the MLSS concentration can be accomplished through several methods. One approach involves augmenting the rate at which excess sludge is removed from the wastewater system. This includes regulating the rate or frequency of sludge wasting to maintain the desired MLSS levels (Advent Envirocare Technology, n.d.).

Next, the calculated SVI of 12.98 mL/g in this study was found to deviate from the typical operational range of 50 mL/g to 150 mL/g. This suggested that the sludge generated in this study was dense and exhibited rapid settling characteristics. Such behaviour was often associated with aged and over-oxidized sludge commonly found in extended aeration facilities. As this type of sludge settled, it produced a cloudy appearance in the supernatant above the settled sludge blanket, a phenomenon known as pinpoint floc (pin-floc). The sludge typically settled swiftly after the commencement of the

settleability test, without forming larger particles prior to settling. While effluent Biochemical Oxygen Demand (BOD) results may meet requirements, elevated Total Suspended Solids (TSS) levels could still persist (Ken, 2023). To increase the SVI, it is needed to increase the waste sludge rate (rate of excess sludge removal), which in turns lowering the MLSS concentrations. This adjustment will consequently slow down the settling rate while causing more suspended solids to be captured in the mixed liquor. As a result, the effluent would become clearer (Biological Waste Treatment Expert, 2019).

#### 4.8 Comparison of Optimal Parameters with Literatures

After determining the optimal parameters from previous studies, a comparison was conducted with findings from other literature sources to validate the results of this study. Table 4.7 below shows the comparison between optimal parameters obtained in this study with those reported in literatures.

Table 4.7: Comparison of Parameters.

Parameters	Sources		
	This Study	(Abd-Elhakeem, M. Ramadan and S. Basaad, 2016)	(Abdullah and Jaeel, 2019)
Coagulant Dosage	40,000 mg/L	100 mg/L	40 mg/L
Solution pH	7	7	6 - 7
Initial Heavy Metal Concentration	100 mg/L	20 mg/L	5 mg/L
Acids Used	Sulphuric acid	Acetic acid	Acetic acid
Removal Efficiency	96.13 %	99.94 %	99.7 %

From the comparison presented in Table 4.7, it was evident that the solution pH remained consistent at pH 7 across all studies. However, notable disparities were observed in coagulant dosages and initial heavy metal concentrations, possibly influenced by variations in the purity, molecular weight, and deacetylation degree of chitosan utilized. Additionally, both studies employed acetic acid as the chosen acid for the coagulation process. Lastly, the removal efficiency achieved in this study (96.13 %) was comparable with findings from other researches.

## CHAPTER 5

### CONCLUSIONS AND RECOMMENDATIONS

#### 5.1 Conclusions

This study examined the properties of chitosan through FTIR, SEM-EDX, and XRD analyses. FTIR analysis revealed the presence of  $\text{-NH}_2$  and  $\text{-OH}$  groups in chitosan. SEM results depicted a smooth, nonporous membranous structure with dome-shaped orifices, microfibrils, and crystallites. EDX analysis indicated that chitosan primarily comprised C, O, and N.

Various parameters such as chitosan to alum ratio, and type of acids, chitosan dosages, solution pH and initial Ni concentration were investigated to identify optimal conditions. It was found that using chitosan as a standalone coagulant was more effective than using it as a coagulant aid with alum. The optimum conditions for achieving maximum Ni ion removal efficiency were determined as follows: 40 g/L of pure chitosan to treat a wastewater solution with an initial Ni concentration of 100 mg/L, adjusted to  $\text{pH} = 7$  using  $\text{H}_2\text{SO}_4$ . Under these conditions, the Ni removal efficiency reached 96.13 %.

The oxidation treatment process was found capable to reduce the chitosan dosage to as low as 10 g/L during coagulation process. From an economic standpoint, there were significant cost savings as the required amount of chitosan was reduced by a factor of four. The SVI calculated in this study was 12.98 mL/g, suggesting that the sludge generated in this study was dense and exhibited rapid settling characteristics. Fortunately, this problem could be addressed or mitigated in a real wastewater treatment facility due to presence of sludge wasting and filtration processes.

In short, chitosan appears to be a promising green alternative to replace the conventional coagulants in wastewater treatment.

#### 5.2 Recommendations for future work

Acetic acid can be used as it has been identified as the most suitable option for dissolving chitosan, offering an effective means to prepare the solution. During this study, the decision not to utilize acetic acid was prompted by the

absence of available stock of the acid. Additionally, exploiting the increased solubility of chitosan at elevated temperatures provides a strategy for enhancing its dissolution through heating. Sodium hydroxide (NaOH) can also be employed during the coagulation process to boost the removal efficiency of heavy metals. While its primary role is neutralization, resulting in the formation of metal hydroxides, NaOH can still contribute to enhancing the efficiency of heavy metal removal. To further optimize the coagulation process, it could be integrated with an aeration process. This combined approach warrants exploration to determine if it can yield additional improvements in overall coagulation performance and removal efficiency.

## REFERENCES

A. F. Lahiji, F., Bairagi, S., Magnusson, R., Sortica, M.A., Primetzhofer, D., Ekström, E., Paul, B., le Febvrier, A. and Eklund, P., 2023. Growth and optical properties of NiO thin films deposited by pulsed dc reactive magnetron sputtering. *Journal of Vacuum Science & Technology A*, 41(6). <https://doi.org/10.1116/6.0002914>.

Abd-Elhakeem, M.A., M. Ramadan, M. and S. Basaad, F., 2016. Removing of heavymetals from water by chitosan nanoparticles. *JOURNAL OF ADVANCES IN CHEMISTRY*, 11(7), pp.3765–3771. <https://doi.org/10.24297/jac.v11i7.2200>.

Abdullah Al Balushi, K.S., Devi, G., Rashid Khamis Al Gharibi, A.S., Adeeb, M.A.S., Al Hudaifi, A.S.M. and Khalfan Al Shabibi, S.S., 2021. Extraction of bio polymers from crustacean shells and its application in refinery wastewater treatment. *Walailak Journal of Science and Technology*, 18(5), pp.1–11. <https://doi.org/10.48048/wjst.2021.11543>.

Abdullah, H.A. and Jaeel, A.J., 2019. Chitosan as a Widely Used Coagulant to Reduce Turbidity and Color of Model Textile Wastewater Containing an Anionic Dye (Acid Blue). *IOP Conference Series: Materials Science and Engineering*, [online] 584(1), pp.12–36. <https://doi.org/10.1088/1757-899X/584/1/012036>.

Advent Envirocare Technology, n.d. *OPTIMISING OPERATIONS OF YOUR ACTIVATED SLUDGE PLANT*.

Alazaiza, M., Albahnasawi, A., Al-Maskari, O., Al Maskari, T., Abujazar, M., Abu Amr, S. and Nassani, D.E., 2022. Role of natural coagulants in the removal of heavy metals from different wastewaters: principal mechanisms, applications, challenges, and prospects. *Global Nest Journal*, 24(4), pp.594–606. <https://doi.org/10.30955/gnj.004478>.

Alazaiza, M.Y.D., Albahnasawi, A., Ali, G.A.M., Bashir, M.J.K., Nassani, D.E., Al Maskari, T., Amr, S.S.A. and Abujazar, M.S.S., 2022. Application of Natural Coagulants for Pharmaceutical Removal from Water and Wastewater: A Review. *Water*, [online] 14(2), p.140. <https://doi.org/10.3390/w14020140>.

Al-Enezi, G., Hamoda, M.F. and Fawzi, N., 2004. Ion Exchange Extraction of Heavy Metals from Wastewater Sludges. *Journal of Environmental Science and Health, Part A*, [online] 39(2), pp.455–464. <https://doi.org/10.1081/ESE-120027536>.

Al-Hussein, A., 2021. Using sulfuric acid (H<sub>2</sub>SO<sub>4</sub>) for pH adjustment in water treatment. *Journal of Petroleum Research and Studies*, 11, pp.19–27. <https://doi.org/10.52716/jprs.v11i3.530>.

APIS, 2016. *Heavy Metals*. [online] UK Centre for Ecology & Hydrology. Available at: <[https://www.apis.ac.uk/overview/pollutants/overview\\_hm.htm#:~:text=As%20they%20are%20elements%2C%20heavy,lake%2C%20estuarine%20or%20marine%20sediments.](https://www.apis.ac.uk/overview/pollutants/overview_hm.htm#:~:text=As%20they%20are%20elements%2C%20heavy,lake%2C%20estuarine%20or%20marine%20sediments.)> [Accessed 7 July 2023].

Bahrodin, M.B., Zaidi, N.S., Hussein, N., Sillanpää, M., Prasetyo, D.D. and Syafiuddin, A., 2021. Recent Advances on Coagulation-Based Treatment of Wastewater: Transition from Chemical to Natural Coagulant. *Current Pollution Reports*, [online] 7(3), pp.379–391. <https://doi.org/10.1007/s40726-021-00191-7>.

Barrera-Díaz, C.E., Balderas-Hernández, P. and Bilyeu, B., 2018. Chapter 3 - Electrocoagulation: Fundamentals and Prospectives. In: C.A. Martínez-Huitle, M.A. Rodrigo and O. Scialdone, eds. *Electrochemical Water and Wastewater Treatment*. [online] Butterworth-Heinemann. pp.61–76. <https://doi.org/https://doi.org/10.1016/B978-0-12-813160-2.00003-1>.

Bazrafshan, E., Kord Mostafapour, F., Alizadeh, M. and Farzadkia, M., 2016. Dairy wastewater treatment by chemical coagulation and adsorption on modified dried activated sludge: a pilot-plant study. *Desalination and Water Treatment*, [online] 57(18), pp.8183–8193. <https://doi.org/10.1080/19443994.2015.1018331>.

Bazrafshan, E., Mohammadi, L., Ansari-Moghaddam, A. and Mahvi, A.H., 2015. Heavy metals removal from aqueous environments by electrocoagulation process— a systematic review. *Journal of Environmental Health Science and Engineering*, [online] 13(74). <https://doi.org/10.1186/s40201-015-0233-8>.

Bina, B., Mehdinejad, M., Nikaeen, M. and Attar, M., 2009. Effectiveness of chitosan as natural coagulant aid in treating turbid waters. *Journal of Environmental Health Science and Engineering*, 6(4), pp.247–252.

Biological Waste Treatment Expert, 2019. *What does having a high SVI mean for Return (RAS) and Waste (WAS) in activated sludge*. [online] Available at: <<https://www.biologicalwasteexpert.com/blog/what-does-having-a-high-svi-mean-for-return-ras-and-waste-was-in-activated-sludge#:~:text=Poor%20settling%20and%20compacting%20sludge,in%20the%20RAS%20%26%20WAS%20lines.>> [Accessed 4 April 2024].

Brandt, M.J., Johnson, K.M., Elphinston, A.J. and Ratnayaka, D.D., 2017. Chapter 8 - Storage, Clarification and Chemical Treatment. In: M.J. Brandt, K.M. Johnson, A.J. Elphinston and D.D. Ratnayaka, eds. *Twort's Water Supply (Seventh Edition)*. [online] Boston: Butterworth-Heinemann. pp.323–366. <https://doi.org/https://doi.org/10.1016/B978-0-08-100025-0.00008-9>.

Brian, C., 2022. *What is Coagulation for Water Treatment?* [online] Available at: <<https://www.wwdmag.com/what-is-articles/article/10940184/what-is-coagulation-for-water-treatment>> [Accessed 18 August 2023].

BYJU'S, 2023. *What is pKa?* [online] Available at: <<https://byjus.com/chemistry/pka/#:~:text=pKa%20is%20a%20number%20that,acidity%20of%20a%20particular%20molecule>> [Accessed 26 August 2023].

Chai, L., 2020. The river water quality before and during the Movement Control Order (MCO) in Malaysia. *Case Studies in Chemical and Environmental Engineering*, [online] 2, p.100027. <https://doi.org/https://doi.org/10.1016/j.cscee.2020.100027>.

ChemREADY, 2018. *Coagulation In Wastewater Treatment. What is the Purpose?* [online] Available at: <<https://www.getchemready.com/water-facts/what-is-purpose-of-coagulation-in-wastewater-treatment/#:~:text=The%20primary%20purpose%20of%20using,in%20the%20water%20are%20neutralized.>> [Accessed 18 August 2023].

ChemREADY, 2023. *pH Adjusters for Water Treatment.* [online] Available at: <<https://www.getchemready.com/ph-adjusters-for-water-treatment/#:~:text=What%20chemicals%20are%20used%20to,application%20the%20more%20heat%20generated.>> [Accessed 26 August 2023].

Chemtech, 2020. *HOW TO CALCULATE AND CONTROL SLUDGE VOLUME INDEX (SVI).* [online] Available at: <<https://chemtech-us.com/articles/how-to-calculate-and-control-sludge-volume-index-svi/>> [Accessed 19 April 2024].

Chen, Q., Yao, Y., Li, X., Lu, J., Zhou, J. and Huang, Z., 2018. Comparison of heavy metal removals from aqueous solutions by chemical precipitation and characteristics of precipitates. *Journal of Water Process Engineering*, [online] 26, pp.289–300. <https://doi.org/https://doi.org/10.1016/j.jwpe.2018.11.003>.

Dahman, Y., 2017. Chapter 6 - Nanopolymers\*\*By Yaser Dahman, Kevin Deonanan, Timothy Dontosos, and Andrew Iammatteo. In: Y. Dahman, ed. *Nanotechnology and Functional Materials for Engineers*. [online] Elsevier. pp.121–144. <https://doi.org/https://doi.org/10.1016/B978-0-323-51256-5.00006-X>.

Das, N., Rajput, H., Aly Hassan, A. and Kumar, S., 2023. Application of Different Coagulants and Cost Evaluation for the Treatment of Oil and Gas Produced Water. *Water*, [online] 15(3), p.464. <https://doi.org/10.3390/w15030464>.

Department of Environment, 2010. *Environmental Requirements: A Guide For Investors*. 11th ed. [online] Putrajaya: Department of Environment, Ministry of Natural Resources and Environment, Malaysia. Available at: <<https://enviro2.doe.gov.my/ekmc/wp-content/uploads/2016/08/1403056822-A%20Guide%20For%20Investors%20-%202010.pdf>> [Accessed 5 July 2023].



- Eric, B., 2022. *WASTEWATER COAGULATION*. [online] Available at: <<https://www.dober.com/water-treatment/resources/wastewater-coagulation#:~:text=Coagulation%20is%20the%20chemical%20water,or%20oily%20materials%20in%20suspension.>> [Accessed 18 August 2023].
- Fan, J., Chen, Q., Li, J., Wang, D., Zheng, R., Gu, Q. and Zhang, Y., 2019. Preparation and Dewatering Property of Two Sludge Conditioners Chitosan/AM/AA and Chitosan/AM/AA/DMDAAC. *Journal of Polymers and the Environment*, [online] 27(2), pp.275–285. <https://doi.org/10.1007/s10924-018-1342-0>.
- Fernandes, Q.M., Melo, K.R.T., Sabry, D.A., Sasaki, G.L. and Rocha, H.A.O., 2015. Does the Use of Chitosan Contribute to Oxalate Kidney Stone Formation? *Marine Drugs*, [online] 13(1), pp.141–158. <https://doi.org/10.3390/md13010141>.
- Fu, Z.-J., Jiang, S.-K., Chao, X.-Y., Zhang, C.-X., Shi, Q., Wang, Z.-Y., Liu, M.-L. and Sun, S.-P., 2022. Removing miscellaneous heavy metals by all-in-one ion exchange-nanofiltration membrane. *Water Research*, [online] 222, pp.43–1354. <https://doi.org/https://doi.org/10.1016/j.watres.2022.118888>.
- Genesis Water Tech, 2019. *8 Painful Points of Chemical Coagulation Treatment Plants*. [online] Available at: <<https://genesiswatertech.com/blog-post/8-painful-points-of-chemical-coagulation-treatment-plants/#:~:text=Due%20to%20the%20sludge%20and,treatment%2C%20and%20the%20disposal%20itself.>> [Accessed 26 August 2023].
- Guibal, E., Vincent, T. and Navarro, R., 2014. Metal ion biosorption on chitosan for the synthesis of advanced materials. *Journal of Materials Science*, [online] 49(16), pp.5505–5518. <https://doi.org/10.1007/s10853-014-8301-5>.
- HariPriyan, U., Gopinath, K.P. and Arun, J., 2022. Chitosan based nano adsorbents and its types for heavy metal removal: A mini review. *Materials Letters*, [online] 312, p.131670. <https://doi.org/https://doi.org/10.1016/j.matlet.2022.131670>.
- Hesami, F., Bina, B. and Ebrahimi, A., 2014. The effectiveness of chitosan as coagulant aid in turbidity removal from water. *International Journal of Environmental Health Engineering (IJEHE)*, [online] 3, p.8. <https://doi.org/10.4103/2277-9183.131814>.
- Huang, C.-H., Shen, S.-Y., Dong, C.-D., Kumar, M. and Chang, J.-H., 2020. Removal Mechanism and Effective Current of Electrocoagulation for Treating Wastewater Containing Ni(II), Cu(II), and Cr(VI). *Water*, [online] 12(9). <https://doi.org/10.3390/w12092614>.
- Janyasuthwiong, S., 2017. Bioprecipitation - A Promising Technique for Heavy Metal Removal and Recovery from Contaminated Wastewater Streams. *MOJ Civil Engineering*, 2. <https://doi.org/10.15406/mojce.2017.02.00052>.

Jarup, L., 2003. Hazards of heavy metal contamination. *British Medical Bulletin*, 68, pp.167–182. <https://doi.org/10.1093/bmb/ldg032>.

Jennifer, B., 2023. *Aeration and Oxidation In Well Water Treatment Explained*. [online] Available at: <<https://waterfilterguru.com/aeration-oxidation-in-well-water-treatment/>> [Accessed 20 April 2024].

John, K.K., Tubadi, D.J., Bampole, L.D., Kaniki, T.A., Kanda, N.J.M. and Lukumu, M.E., 2020. Extraction and characterization of chitin and chitosan from *Termitomyces titanicus*. *SN Applied Sciences*, [online] 2(3), p.406. <https://doi.org/10.1007/s42452-020-2186-5>.

Jon, G., 2022. *How are coagulants and flocculants used in water and wastewater treatment?* [online] Available at: <<https://www.wcs-group.co.uk/wcs-blog/coagulants-flocculants-wastewater-treatment>> [Accessed 18 August 2023].

Julkapli, N.M., Ahmad, Z. and Akil, H.M., 2010. X-Ray Diffraction Studies of Cross Linked Chitosan With Different Cross Linking Agents For Waste Water Treatment Application. *AIP Conference Proceedings*, [online] 1202(1), pp.106–111. <https://doi.org/10.1063/1.3295578>.

Ken, T., 2023. *HOW TO CALCULATE SLUDGE VOLUME INDEX – SVI*. [online] Available at: <<https://www.waterandwastewatercourses.com/calculate-sludge-volume-index-svi/>> [Accessed 4 April 2024].

Kevin, C., 2022. *What is a good MLSS value?* [online] Available at: <<https://spertasystems.com/what-is-a-good-mlss-value/>> [Accessed 4 April 2024].

Khairul, N., Rohani, R., Izni, Y.I., Kamsol, M.A., Basiron, S.A. and Abd. Rashid, A.I., 2021. Eco-Friendly Coagulant versus Industrially Used Coagulants: Identification of Their Coagulation Performance, Mechanism and Optimization in Water Treatment Process. *International Journal of Environmental Research and Public Health*, [online] 18(17). <https://doi.org/10.3390/ijerph18179164>.

Kikuchi, T. and Tanaka, S., 2012. Biological Removal and Recovery of Toxic Heavy Metals in Water Environment. *Critical Reviews in Environmental Science and Technology*, [online] 42(10), pp.1007–1057. <https://doi.org/10.1080/10643389.2011.651343>.

Al Kindi, G.Y., Gomaa, G.F. and Abd ulkareem, F.A., 2020. Combined adsorbent best (chemical and natural) coagulation process for removing some heavy metals from wastewater. *International Journal of Environmental Science and Technology*, [online] 17(7), pp.3431–3448. <https://doi.org/10.1007/s13762-020-02702-3>.

Kinuthia, G.K., Ngure, V., Beti, D., Lugalia, R., Wangila, A. and Kamau, L., 2020. Levels of heavy metals in wastewater and soil samples from open drainage channels in Nairobi, Kenya: community health implication. *Scientific Reports*, [online] 10(1), p.8434. <https://doi.org/10.1038/s41598-020-65359-5>.

Kučera, T. and Hofmanová, L., 2020. Moringa Oleifera seeds and Chitosan as alternatives to conventional coagulation agents. In: *IOP Conference Series: Materials Science and Engineering*. Institute of Physics Publishing. <https://doi.org/10.1088/1757-899X/800/1/012032>.

Lara, P.A., Rodríguez, D.C. and Peñuela, G.A., 2016. Application of coagulation by sweep for removal of metals in natural water used in dairy cattle. *Afinidad. Journal of Chemical Engineering Theoretical and Applied Chemistry*, [online] 73(576). Available at: <<https://raco.cat/index.php/afinidad/article/view/318425>>.

Li, B., Elango, J. and Wenhui, W., 2020. Recent Advancement of Molecular Structure and Biomaterial Function of Chitosan from Marine Organisms for Pharmaceutical and Nutraceutical Application. *Applied Sciences*, 10(14), p.4719. <https://doi.org/10.3390/app10144719>.

Lichtfouse, E., Morin-Crini, N., Fourmentin, M., Zemmouri, H., do Carmo Nascimento, I.O., Queiroz, L.M., Tadza, M.Y.M., Picos-Corrales, L.A., Pei, H., Wilson, L.D. and Crini, G., 2019. Chitosan for direct bioflocculation of wastewater. *Environmental Chemistry Letters*, [online] 17(4), pp.1603–1621. <https://doi.org/10.1007/s10311-019-00900-1>.

Machado, C.A., Esteves, A.F. and Pires, J.C.M., 2024. Chlorella vulgaris Harvesting: Chemical Flocculation with Chitosan, Aluminum Sulfate, and Ferric Sulfate. *Applied Sciences*, 14(2), p.598. <https://doi.org/10.3390/app14020598>.

Marei, A., 2019. Effectiveness of chitosan as a natural coagulant in treating turbid waters. *Bionatura*, 4, pp.856–860. <https://doi.org/10.21931/RB/2019.04.02.7>.

Mohamed, R.M., Ismail, A.A., Kini, G., Ibrahim, I.A. and Koopman, B., 2009. Synthesis of highly ordered cubic zeolite A and its ion-exchange behavior. *Colloids and Surfaces A: Physicochemical and Engineering Aspects*, 348(1–3), pp.87–92. <https://doi.org/10.1016/j.colsurfa.2009.06.038>.

Molly, K., 2021. *Shells for Weight Loss? Here's the Science Behind Chitosan Supplements*. [online] Available at: <<https://www.healthline.com/nutrition/chitosan-supplements>> [Accessed 7 July 2023].

Murtaza, H.A., Mukhangaliyeva, A., Golman, B., Perveen, A. and Talamona, D., 2023. Quantitative Characterization of Metal Powder Morphology, Size Distribution, and Flowability for Additive Manufacturing. *Journal of Materials Engineering and Performance*. [online] <https://doi.org/10.1007/s11665-023-08761-0>.

Nath, A., Mishra, A. and Pande, P.P., 2021. A review natural polymeric coagulants in wastewater treatment. *Materials Today: Proceedings*, [online] 46, pp.6113–6117. <https://doi.org/https://doi.org/10.1016/j.matpr.2020.03.551>.

Nguyen, V.-C.-N., Phan, H.-V.-T., Nguyen, V.-K., Vo, D.-T., Tran, T.-N., Dao, M.-T. and Hoang, L.-T.-T.-T., 2023. A Comparison of a Conventional Chemical Coagulant and a Natural Coagulant Derived from Cassia fistula Seeds for the Removal of Heavy Metal Ions. *Archives of Environmental Contamination and Toxicology*, [online] 85(3), pp.324–331. <https://doi.org/10.1007/s00244-023-01005-1>.

Pang, F.M., Teng, S.P., Teng, T.T. and Omar, A.K.M., 2009. Heavy Metals Removal by Hydroxide Precipitation and Coagulation-Flocculation Methods from Aqueous Solutions. *Water Quality Research Journal*, [online] 44(2), pp.174–182. <https://doi.org/10.2166/wqrj.2009.019>.

Pinotti, A., Bevilacqua, A. and Zaritzky, N., 1999. *Treatment of Anionic Emulsion Systems Using Chitosan, Polyacrylamide, and Aluminum Sulfate*.

Purohit, G. and Rawat, D.S., 2022. Characterization Techniques for Chitosan and Its Based Nanocomposites. In: S. Gulati, ed. *Chitosan-Based Nanocomposite Materials: Fabrication, Characterization and Biomedical Applications*. [online] Singapore: Springer Nature Singapore. pp.79–101. [https://doi.org/10.1007/978-981-19-5338-5\\_3](https://doi.org/10.1007/978-981-19-5338-5_3).

Qasem, N.A.A., Mohammed, R.H. and Lawal, D.U., 2021. Removal of heavy metal ions from wastewater: a comprehensive and critical review. *npj Clean Water*, [online] 4(36), pp.2–6. <https://doi.org/10.1038/s41545-021-00127-0>.

Rahman, A., Haque, M.A., Ghosh, S., Shinu, P., Attimarad, M. and Kobayashi, G., 2023. Modified Shrimp-Based Chitosan as an Emerging Adsorbent Removing Heavy Metals (Chromium, Nickel, Arsenic, and Cobalt) from Polluted Water. *Sustainability (Switzerland)*, 15(3). <https://doi.org/10.3390/su15032431>.

Rajoria, S., Vashishtha, M. and Sangal, V.K., 2022. Treatment of electroplating industry wastewater: a review on the various techniques. *Environmental Science and Pollution Research*, [online] 29(48), pp.72196–72246. <https://doi.org/10.1007/s11356-022-18643-y>.

Randive, P.S., Singh, D.P., Bhole, A.G., Varghese, V.P. and Badar, A.M., 2021. Evaluation of Fractal Growth Characteristic of Floccs for Aluminium Sulphate and Ferric Chloride Using Microscopy Method. In: L.M. Gupta, M.R. Ray and P.K. Labhassetwar, eds. *Advances in Civil Engineering and Infrastructural Development*. Singapore: Springer Singapore. pp.487–494.

ResearchAndMarkets, 2018. *Malaysia Metal Finishing Chemicals Market Analysis, Companies Profiles, Size, Share, Growth, Trends & Forecast to 2025*. [online] Available at: <<https://www.businesswire.com/news/home/20180427005264/en/Malaysia-Metal-Finishing-Chemicals-Market-Analysis-Companies-Profiles-Size-Share-Growth-Trends-Forecast-to-2025---ResearchAndMarkets.com>> [Accessed 18 February 2024].

Ron, T., 2010. *What the Heck Is SVI?* [online] Available at: <<https://www.tpomag.com/editorial/2010/03/what-the-heck-is-svi>> [Accessed 4 April 2024].

Rosińska, A. and Dąbrowska, L., 2021. Influence of type and dose of coagulants on effectiveness of PAH removal in coagulation water treatment. *Water Science and Engineering*, [online] 14(3), pp.193–200. <https://doi.org/https://doi.org/10.1016/j.wse.2021.08.004>.

Sajid, M., 2023. *Hydrochloric acid vs. Sulfuric acid: The Differences*. [online] Available at: <[https://psiberg.com/hydrochloric-acid-vs-sulfuric-acid/#google\\_vignette](https://psiberg.com/hydrochloric-acid-vs-sulfuric-acid/#google_vignette)> [Accessed 26 August 2023].

Saleha, K., 2023. *What is mixed liquor suspended solids?* [online] Available at: <<https://www.wwdmag.com/what-is-articles/article/33011991/what-is-mixed-liquor-suspended-solids>> [Accessed 19 April 2024].

Saritha, V., Srinivas, N. and Srikanth Vuppala, N. V, 2017. Analysis and optimization of coagulation and flocculation process. *Applied Water Science*, [online] 7(1), pp.451–460. <https://doi.org/10.1007/s13201-014-0262-y>.

Sarup, R., Behl, K., Joshi, M. and Nigam, S., 2021. Chapter 18 - Heavy metal removal by cyanobacteria. In: M.P. Shah, S. Rodriguez Couto and V. Kumar, eds. *New Trends in Removal of Heavy Metals from Industrial Wastewater*. [online] Elsevier. pp.441–466. <https://doi.org/https://doi.org/10.1016/B978-0-12-822965-1.00018-0>.

SDC, 2017. *What is Electroplating?* [online] Available at: <<https://www.sharrettsplating.com/blog/what-electroplating/>> [Accessed 5 July 2023].

Shammas, N.K., Hahn, H.H., Wang, M.-H.S. and Wang, L.K., 2021. Fundamentals of Chemical Coagulation and Precipitation. In: L.K. Wang, M.-H.S. Wang, N.K. Shammas and D.B. Aulenbach, eds. *Environmental Flotation Engineering*. [online] Cham: Springer International Publishing. pp.95–142. [https://doi.org/10.1007/978-3-030-54642-7\\_3](https://doi.org/10.1007/978-3-030-54642-7_3).

Sourav, B., 2023. *Membrane Filtration Method, Types, Advantages, Disadvantages, Applications*. [online] Available at: <<https://microbiologynote.com/membrane-filtration-method-types-advantages-disadvantages-applications/>> [Accessed 6 August 2023].

Stephen, L., 2023. Acid-Base Gallery. In: *Chem1 Virtual Textbook*. [online] Vancouver: LibreTexts Chemistry. pp.515–525. Available at: <<https://www.chem1.com/acad/webtext/virtualtextbook.html>> [Accessed 26 August 2023].

Subbaiah, M.P. and Sankaran, M., 2021. Synthesis and Modification Strategies of Chitosan and Its Interaction with Metal Ions. In: R. Jayakumar and M. Prabaharan, eds. *Chitosan for Biomaterials III: Structure-Property Relationships*. [online] Cham: Springer International Publishing. pp.75–104. [https://doi.org/10.1007/12\\_2021\\_88](https://doi.org/10.1007/12_2021_88).

Sumiahadi, A., Acar, R. and Direk, M., 2019. *THE POTENTIAL USE OF COVER CROPS FOR PHYTOREMEDIATION PROCESS OF HEAVY METALS CONTAMINATED SOILS*.

Sun, H., Jiao, R., Xu, H., An, G. and Wang, D., 2019. The influence of particle size and concentration combined with pH on coagulation mechanisms. *Journal of Environmental Sciences*, [online] 82, pp.39–46. <https://doi.org/https://doi.org/10.1016/j.jes.2019.02.021>.

Tahraoui, H., Toumi, S., Boudoukhani, M., Touzout, N., Sid, A.N.E.H., Amrane, A., Belhadj, A.E., Hadjadj, M., Laichi, Y., Aboumustapha, M., Kebir, M., Bouguettoucha, A., Chebli, D., Assadi, A.A. and Zhang, J., 2024. Evaluating the Effectiveness of Coagulation–Flocculation Treatment Using Aluminum Sulfate on a Polluted Surface Water Source: A Year-Long Study. *Water (Switzerland)*, 16(3). <https://doi.org/10.3390/w16030400>.

Takaara, T. and Kurumada, K., 2023. Optimum Conditions for Enhancing Chitosan-Assisted Coagulation in Drinking Water Treatment. *Sustainability (Switzerland)*, 15(19). <https://doi.org/10.3390/su151914197>.

Tang, X., Zheng, H., Teng, H., Sun, Y., Guo, J., Xie, W., Yang, Q. and Chen, W., 2016. Chemical coagulation process for the removal of heavy metals from water: a review. *Desalination and Water Treatment*, [online] 57(4), pp.1733–1748. <https://doi.org/10.1080/19443994.2014.977959>.

Tchounwou, P.B., Yedjou, C.G., Patlolla, A.K. and Sutton, D.J., 2012. Heavy Metal Toxicity and the Environment. In: A. Luch, ed. *Molecular, Clinical and Environmental Toxicology: Volume 3: Environmental Toxicology*. [online] Basel: Springer Basel. pp.133–164. [https://doi.org/10.1007/978-3-7643-8340-4\\_6](https://doi.org/10.1007/978-3-7643-8340-4_6).

Teng, T.T. and Chang, S., 2011. The risks and treatments of heavy metals from electroplating wastewater. *Hazardous Materials: Types, Risks and Control*, pp.315–338.

Thakur, A.K., Kumar, R., Chaudhari, P. and Shankar, R., 2021. Removal of Heavy Metals Using Bentonite Clay and Inorganic Coagulants. In: M.P. Shah, ed. *Removal of Emerging Contaminants Through Microbial Processes*. [online] Singapore: Springer Singapore. pp.47–69. [https://doi.org/10.1007/978-981-15-5901-3\\_3](https://doi.org/10.1007/978-981-15-5901-3_3).

Thermo Fisher Scientific Inc., 2023. *EDX Analysis with a Scanning Electron Microscope (SEM): How does it work?* [online] Available at: <<https://www.thermofisher.com/my/en/home/global/forms/industrial/edx-analysis-sem.html>> [Accessed 20 August 2023].

Toprak Home Page, 2006. *Conventional Water Treatment Processes*. [online] Available at: <<https://web.deu.edu.tr/atiksu/ana52/aryen2.html#:~:text=Two%20important%20factors%20in%20coagulant,pH%208%20under%20some%20conditions.>>> [Accessed 7 July 2023].

VITO, 2020. *Neutralisation*. [online] Available at: <<https://emis.vito.be/en/bat/tools-overview/sheets/neutralisation>> [Accessed 26 August 2023].

Wang, P., Li, L., Pang, X., Zhang, Y., Zhang, Y., Dong, W.F. and Yan, R., 2021. Chitosan-based carbon nanoparticles as a heavy metal indicator and for wastewater treatment. *RSC Advances*, 11(20), pp.12015–12021. <https://doi.org/10.1039/d1ra00692d>.

Water World, 2001. *Alum Replacement Gains Popularity at Municipal Plants*. [online] Available at: <<https://www.waterworld.com/home/article/16191916/alum-replacement-gains-popularity-at-municipal-plants>> [Accessed 7 July 2023].

Wijayati, N., Lestari, L.R., Wulandari, L.A., Mahatmanti, F.W., Rakainsa, S.K., Cahyono, E. and Wahab, R.A., 2021. Potassium Alum [KAl(SO<sub>4</sub>)<sub>2</sub>·12H<sub>2</sub>O] solid catalyst for effective and selective methoxylation production of alpha-pinene ether products. *Heliyon*, 7(1). <https://doi.org/10.1016/j.heliyon.2021.e06058>.

Wong, J.F., Chan, J.X., Hassan, A., Mohamad, Z. and Othman, N., 2020. Functional Chitosan-Based Composites for Potential Application in Food Industry. In: S. Siddiquee, M. Gan Jet Hong and Md. Mizanur Rahman, eds. *Composite Materials: Applications in Engineering, Biomedicine and Food Science*. [online] Cham: Springer International Publishing. pp.431–458. [https://doi.org/10.1007/978-3-030-45489-0\\_21](https://doi.org/10.1007/978-3-030-45489-0_21).

Xiang, H., Min, X., Tang, C.-J., Sillanpää, M. and Zhao, F., 2022. Recent advances in membrane filtration for heavy metal removal from wastewater: A mini review. *Journal of Water Process Engineering*, [online] 49, p.103023. <https://doi.org/https://doi.org/10.1016/j.jwpe.2022.103023>.

Xu, Y., Gan, K., Liang, S., Liu, H. and Wang, Q., 2021. Investigation and optimization of chitosan performance in flocculating kaolin suspensions using a real-time suspending solid concentration measuring method. *Water (Switzerland)*, 13(4). <https://doi.org/10.3390/w13040513>.

Yaneva, Z., Ivanova, D., Nikolova, N. and Tzanova, M., 2020. The 21st century revival of chitosan in service to bio-organic chemistry. *Biotechnology & Biotechnological Equipment*, 34, pp.221–237. <https://doi.org/10.1080/13102818.2020.1731333>.

Zhang, L., Zeng, Y. and Cheng, Z., 2016. *Removal of heavy metal ions using chitosan and modified chitosan: A review. Journal of Molecular Liquids*, <https://doi.org/10.1016/j.molliq.2015.12.013>.

Zhou, J., Liu, Y., Li, B., Li, H., Guikui, C. and Qiu, R., 2023. ARTICLE Coagulation of trace arsenic and cadmium from drinking water using titanium potassium oxalate. *npj Clean Water*, 6(9). <https://doi.org/10.1038/s41545-023-00227-z>.



## APPENDICES

### Appendix A: Preparation of Various Molarity of Acids

To determine the molarity of acids (HCl, H<sub>2</sub>SO<sub>4</sub>, and HNO<sub>3</sub>) required for the experiment from a stock solution, a dilution process was essential. This involved knowing the molarity of the stock solution, the desired molarity, and the volume of acid needed. The required volume from the stock solution could then be calculated by using:

$$M_1V_1 = M_2V_2$$

where

$M_1$  = molarity of stock's solution, M

$V_1$  = volume of stock solution, mL

$M_2$  = molarity of diluted solution, M

$V_2$  = volume of diluted solution, mL

Given that the principle and calculation remained consistent across all acids, only one sample calculation will be demonstrated, utilizing the preparation of 1M HCl.

$$\begin{aligned}M_1V_1 &= M_2V_2 \\(12.08 \text{ M})V_1 &= (1\text{M})(1000 \text{ mL}) \\V_1 &= 82.8 \text{ mL}\end{aligned}$$

Therefore, 82.8 mL of 37 % HCl stock solution was pipetted and then diluted by adding distilled water until the volume reached 1000 mL.

Table A-1: Volume of HCl Stock Solutions Required to Prepare Different Molarity of HCl in 1000 mL.

<b>Molarity of HCl (M)</b>	<b>Volume of 37 % HCl Stock Solution Required (mL)</b>
1	82.8
0.1	8.28

Table A-2: Volume of H<sub>2</sub>SO<sub>4</sub> Stock Solutions Required to Prepare Different Molarity of H<sub>2</sub>SO<sub>4</sub> in 1000 mL.

<b>Molarity of H<sub>2</sub>SO<sub>4</sub> (M)</b>	<b>Volume of 95 % H<sub>2</sub>SO<sub>4</sub> Stock Solution Required (mL)</b>
1	56.2
0.1	5.62

Table A-3: Volume of HNO<sub>3</sub> Stock Solutions Required to Prepare Different Molarity of HNO<sub>3</sub> in 1000 mL.

<b>Molarity of HNO<sub>3</sub> (M)</b>	<b>Volume of 65 % HNO<sub>3</sub> Stock Solution Required (mL)</b>
1	71.4
0.1	7.14

## Appendix B: Preparation of Nickel Standards for ICP-OES

To create the calibration curve for nickel in ICP-OES, it was necessary to prepare nickel standards with various concentrations from a stock solution. This process involved determining the concentration of the stock solution, the desired concentration, and the volume of standards required. The volume needed from the stock solution could then be calculated using:

$$C_1V_1 = C_2V_2$$

where

$C_1$  = concentration of stock's solution, mg/L

$V_1$  = volume of stock solution, mL

$C_2$  = concentration of diluted solution, mg/L

$V_2$  = volume of diluted solution, mL

To prevent contamination of the original stock solution, an intermediate stock solution of 400 mg/L was prepared, and subsequent standards were made using this intermediate solution.

$$C_1V_1 = C_2V_2$$

$$(1000 \text{ mg/L})V_1 = (400 \text{ mg/L})(100 \text{ mL})$$

$$V_1 = 40 \text{ mL}$$

Therefore, 40 mL of 1000 mg/L nickel stock solution was pipetted and then diluted by adding deionized water until the volume reached 100 mL. Next, a nickel standard solution of 50 mg/L was prepared.

$$C_1V_1 = C_2V_2$$

$$(400 \text{ mg/L})V_1 = (50 \text{ mg/L})(50 \text{ mL})$$

$$V_1 = 6.25 \text{ mL}$$

Table B-1: Volume of Nickel Intermediate Solutions Required to Prepare Different Concentrations of Nickel Standards.

Concentration of Nickel Standards (mg/L)	Volume of 400 mg/L Nickel Intermediate Solution Required (mL)
50	6.25
100	12.50
150	18.75
200	25.00
250	31.25

### Ni 231.604

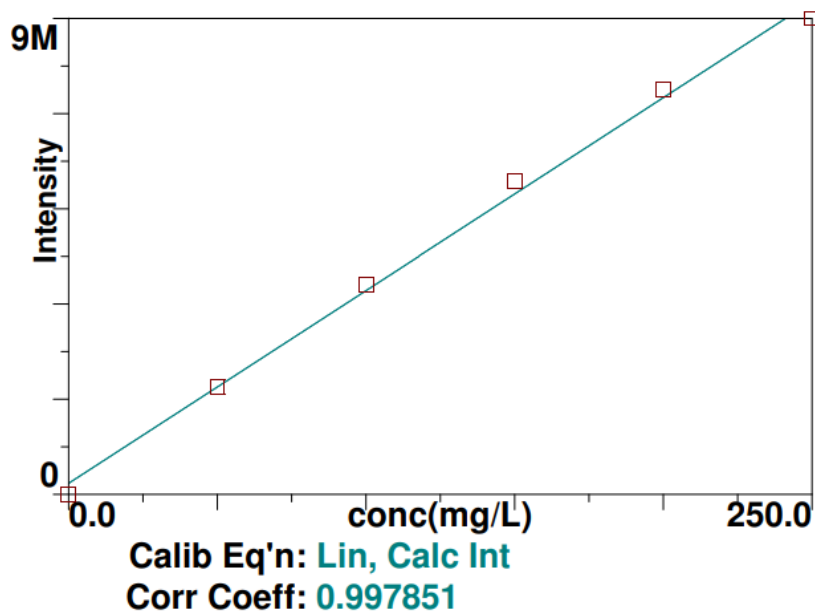


Figure B-1: ICP-OES Calibration Curve of Nickel at 0 mg/L to 250 mg/L.

### Appendix C: Calculation for Sludge Volume Index and Mixed Liquor Suspended Solids.

Before SVI can be determined, it was required to calculate the MLSS first. This process involved determining the initial and final weight of filter paper as well as the volume of sample used. Then, the MLSS value can be calculated by using the equation below:

$$\text{MLSS} = \frac{(W_f - W_i) \times 1000 \times 1000}{\text{Volume of Sample (mL)}}$$

where

MLSS = mixed liquor suspended solids, mg/L

$W_f$  = final weight of filter paper, g

$W_i$  = initial weight of filter paper, g

$$\text{SVI (mL/g)} = \frac{\text{Settled Sludge Volume (mL/L)} \times 1000 \text{ mg/g}}{\text{Mixed Liquor Suspended Solids, MLSS (mg/L)}}$$

Once the initial and final weight of filter paper was determined, the MLSS value can be calculated.

$$\begin{aligned} \text{MLSS} &= \frac{(W_f - W_i) \times 1000 \times 1000}{\text{Volume of Sample (mL)}} \\ \text{MLSS} &= \frac{(0.9109 \text{ g} - 0.5103 \text{ g}) \times 1000 \times 1000}{50 \text{ mL}} \\ \text{MLSS} &= 8012 \text{ mg/L} \end{aligned}$$

With this, the SVI can then be calculated as well:

$$\begin{aligned} \text{SVI} &= \frac{\text{Settled Sludge Volume (mL/L)} \times 1000 \text{ mg/g}}{\text{Mixed Liquor Suspended Solids, MLSS (mg/L)}} \\ \text{SVI} &= \frac{104 \text{ mL/L} \times 1000 \text{ mg/g}}{8012 \text{ mg/L}} \\ \text{SVI} &= 12.98 \text{ mL/g} \end{aligned}$$